2012

Microarray-based identification of Pitx3 targets during Xenopus embryogenesis

L Hooker

C Smoczer

Farhad Khosrowshahian
University of Windsor

Michael J. Crawford
University of Windsor

DEVELOPMENTAL DYNAMICS 241:1487–1505, 2012

PATTERNS & PHENOTYPES

Microarray-Based Identification of Pitx3 Targets During *Xenopus* Embryogenesis

Lara Hooker, Cristine Smoczer, Farhad KhosrowShahian, Marian Wolanski, and Michael J. Crawford*

Background: Unexpected phenotypes resulting from morpholino-mediated translational knockdown of *Pitx3* in *Xenopus laevis* required further investigation regarding the genetic networks in which the gene might play a role. Microarray analysis was, therefore, used to assess global transcriptional changes downstream of *Pitx3*. Results: From the large data set generated, selected candidate genes were confirmed by reverse transcriptase-polymerase chain reaction (RT-PCR) and in situ hybridization. Conclusions: We have identified four genes as likely direct targets of Pitx3 action: *Pax6*, β *Crystallin-b1* (*Crybb1*), *Hes7.1*, and *Hes4*. Four others show equivocal promise worthy of consideration: *Vent2*, and *Ripply2* (aka *Ledgerline* or *Stripy*), *eFGF* and *RXRα*. We also describe the expression pattern of additional and novel genes that are Pitx3-sensitive but that are unlikely to be direct targets. *Developmental Dynamics 241:1487–1505, 2012*. © 2012 Wiley Periodicals, Inc.

Key words: microarray; Pitx3; morpholino; *Xenopus laevis*; eye; lens; somite; Pax6; segmentation clock; retinoid; mutant

Key findings:

- A microarray assay and secondary confirmation of Pitx3 morphants indicates that *Pax6*, β *Crystallin-b1 (Crybb1), Hes7.1*, and *Hes4* are good candidates for direct targets.
- Four other genes show equivocal promise worthy of consideration: *Vent2*, and *Ripply2* (aka *Ledgerline* or *Stripy*), *eFGF* and *RXRα*.
- Novel genes described (but that are likely indirectly affected) are described: *Rbp4l, Galectin IX, Baz2b*, and *Rdh16*.
- In addition to previously described interactions in lens and brain, *Pitx3* also intersects the segmentation pathway and retinoid regulation.

Accepted 9 July 2012

INTRODUCTION

Pitx3 encodes a *bicoid*-like transcription factor that is characterized by a lysine residue at position 50 of the homeodomain. The *aphakia* (*ak*) mouse represents a natural *Pitx3* mutant model that is the result of two deletions in its regulatory region that abolish eye and brain expression, but leave muscle expression intact (Semina et al., 2000; Rieger et al., 2001; Coulon et al., 2007). This genotype displays microphthalmic eyes that lack developed lenses. They also display impaired differentiation of dopaminergic neurons in the *substantia nigra*: mutants mimic the symptoms of Parkinson's disease (PD; Varnum and Stevens, 1968; van den Munckhof et al., 2003). In humans, *PITX3* disruption can lead to congenital cataracts, anterior segment mesenchymal dysgenesis (ASMD), Peter's anomaly, and/ or microphthalmia (Sakazume et al., 2007). This implicates *PITX3* as a major player in the control of gene transcription in lens fibers. In the ventral tegmental area (VTA) and *substantia nigra compacta* (SNc)

Department of Biological Sciences, University of Windsor, Windsor, Ontario, Canada
Grant sponsor: Natural Science and Engineering Research Council of Canada; Grant number: 203459.
***Correspondence to: Michael J. Crawford, Department of Biological Sciences, University of Windsor, 401 Sunset Avenue, Windsor, Ontario, N9B 3P4, Canada. E-mail: mcrawfo@uwindsor.ca**

DOI 10.1002/dvdy.23836
Published online 4 August 2012 in Wiley Online Library (wileyonlinelibrary.com).

J_ID: Z7H Customer A_ID: DVDY23836 Cadmus Art: DVDY23836 Ed. Ref. No.: 12-0073 Date: 4-August-12 Stage: Page: 1488

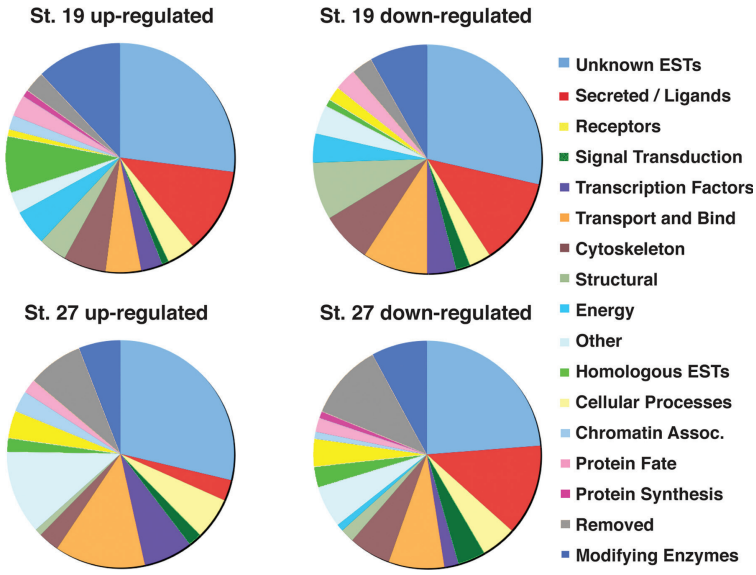

Fig. 1. Microarray data represented according to putative gene function. The 100 most up- and down-regulated transcripts affected by *Pitx3*-morpholino-mediated knockdown were categorized by sequence analysis for stages 19 and 27 of *X. laevis* embryonic development. Colors correspond to functional groups in the legend (right).

regions of the midbrain, *PITX3* is necessary for the terminal differentiation and survival of mesencephalic dopaminergic neurons (mDA; van den Munckhof et al., 2003; Hwang et al., 2009). Zebrafish *pitx3* morphants also exhibit small eyes with lens degeneration, along with misshapen heads, a bent dorsal axis, and reduced jaws and fins (Shi et al., 2005). Disruption of *Pitx3* in *Xenopus laevis* impedes development of lens and retina, and recent evidence suggests an additional role in dorsal axis segmentation and in laterality (Khosrowshahian et al., 2005; Shi et al., 2005; Smoczer et al., In Press). In zebrafish, *Pitx3* expresses in the hypoblast of gastrulating embryos (Dutta et al., 2005), and the transcript is detectable by reverse transcriptase-polymerase chain reaction (RT-PCR) in pregastrula *Xenopus* (Khosrowshahian et al., 2005). These two studies

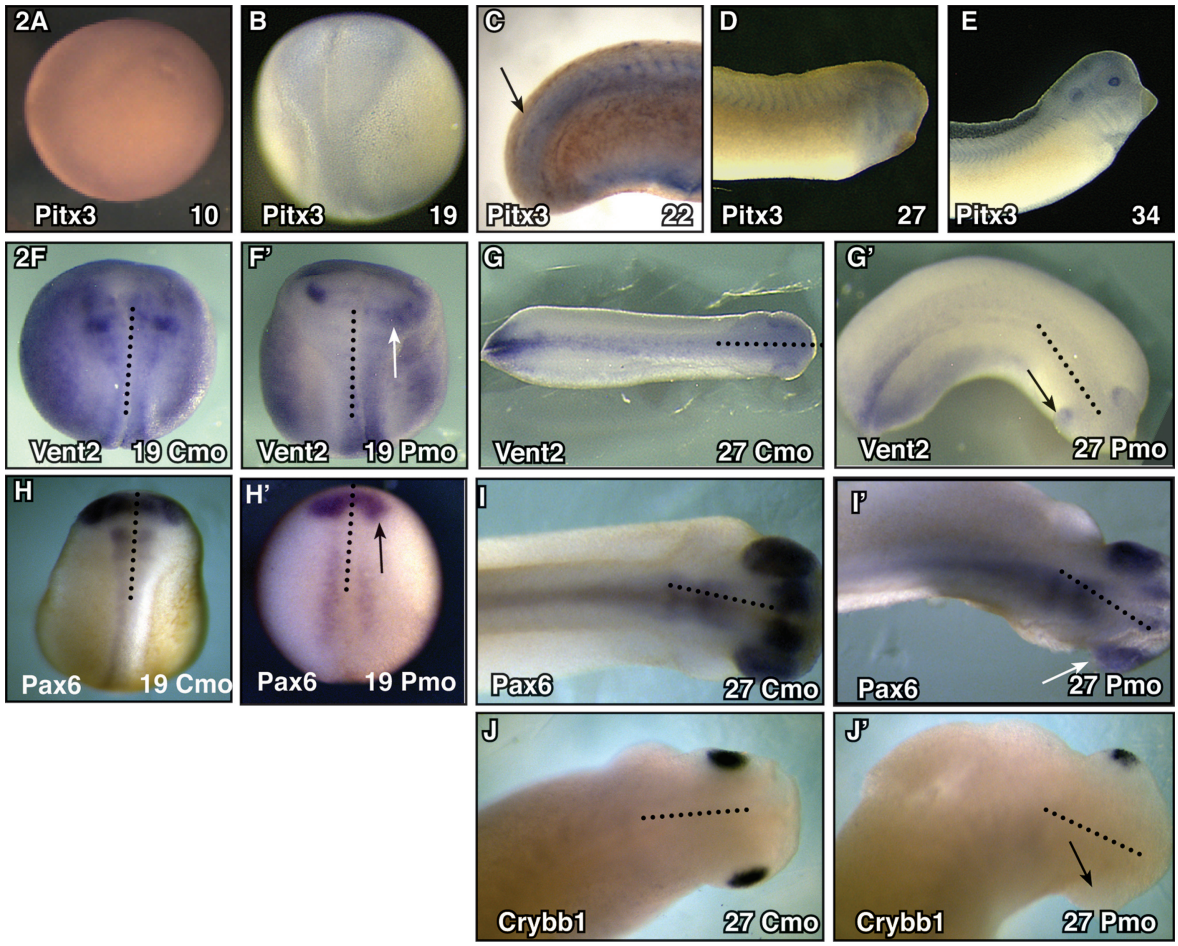

Fig. 2.

ID: manoharj | Black Lining: [ON] | Time: 21:03 | Path: N:/3b2/DVDY/Vol24109/120115/APPFile/JW-DVDY120115

J_ID: Z7H Customer A_ID: DVDY23836 Cadmus Art: DVDY23836 Ed. Ref. No.: 12-0073 Date: 4-August-12 Stage: Page: 1489

suggest an earlier involvement for the gene in dorso-anterior patterning than is generally understood.

Pitx3 binds target DNA to regulate transcription of downstream genes by means of bicoid binding elements (BBE; TAATCC; Lamonerie et al., 1996; Amendt et al., 1998). Pitx3 directly regulates *MIP/Aquaporin O*, which encodes an abundant protein in the lens that functions as an osmotic regulator and cell adhesion molecule (Chepelinsky, 2009; Huang and He, 2010; Sorokina et al., 2011). In zebrafish, pitx3 acts upstream of the transcription factor *foxe3*, which is necessary for the transition of lens epithelial cells into differentiated secondary lens fibers by means of nuclear degradation (Shi et al., 2005). *Pitx3* is also thought to regulate the balance between mitosis and terminal differentiation in the equatorial region of the lens: here, it operates upstream of cell cycle inhibitors *p27Kip1* and *p57Kip2* (Ho et al., 2009). Within midbrain regions, it directly regulates *tyrosine hydroxylase* (*TH*) expression, the rate-limiting enzyme in dopamine production (Landis et al., 1988; Lebel et al., 2001; Messmer et al., 2007). It also controls the neurotransmission of dopamine in mDA neurons by means of regulation of vesicular *monoamine transporter 2* (*VMAT2*) and *dopamine transporter* (*DAT*; Hwang et al., 2009). Direct regulation of *Adh2* in mDA neurons affects the production of retinoic acid that is necessary for proper neuron development (Jacobs et al., 2007). To complicate matters, *Pitx3* is a versatile transcription factor: depending upon signaling context, it can act as either a transcriptional activator or as a repressor (Cazorla et al., 2000; Messmer et al., 2007).

We performed a microarray analysis to compare the transcriptomes of *Pitx3*- and control-morphants at stages 19 (when eye development is commencing) and 27 (when lens differentiation begins; Nieuwkoop and Faber, 1967). We elected to use morpholinos because ectopic expression and dominant negative approaches could affect the response elements of other *Pitx* family members: the ectopic expression approach is impossible to restrict solely to *Pitx3* expression domains, and the homeodomain sequences of Pitx2 and 3, for example, are identical. Pitx2 and 3 differ from Pitx1 by a single amino acid in the turn between helices I and II.

Although the preponderance of literature regarding the gene relates to lens and mDA neurons, *Pitx3* also expresses broadly throughout gastrulation, and later in somites, and lateral plate mesoderm (Pommereit et al., 2001; Khosrowshahian et al., 2005; Smoczer et al., In Press). In zebrafish, *pitx3* expresses in the demarcation of the mesendoderm-derived polster (Dutta et al., 2005). Ectodermal explants have been useful as source material for *Xenopus* microarray experiments in the past, but this restriction to a single germinal layer would miss some likely *Pitx3* targets, and in addition would require the complicating necessity of neural inducing agents. That said, the interpretation of results can also be confounded by the feature that morpholino-mediated translational knockdown, unlike RNAi approaches, solely affects translation and does not appear to affect mRNA degradation rates. Indeed, some embryos are suspected to compensate for morpholino-mediated knockdown by releasing more transcript into circulation (Eisen and Smith, 2008).

We designed our search for *Pitx3* targets to be as broad as possible, and consequently we sampled from whole embryos. The results generated a long list of genes that are affected by *Pitx3* mis-regulation. We characterized novel transcripts that represent putative targets of Pitx3 and report plausible genetic pathways that are regulated by this multifaceted transcription factor.

RESULTS AND DISCUSSION

Microarray Analysis

Morpholino specificity has been previously published and reported to selectively reduce *Pitx3* transcript and protein levels, with the control-morpholino having none of these effects (Khosrowshahian et al., 2005). This specificity has subsequently been confirmed using a second *Pitx3* morpholino and missense control (Smoczer et al., In Press). *Xenopus* microarray GeneChips (Affymetrix) were used, and the data were analyzed comparing control-morpholino treatments to *Pitx3*-morpholino treatments. The threshold for consideration was set at a two-fold cutoff with a P value of < 0.05. We categorized the top 100 up- and down-regulated transcripts at each stage, with regard to function, and generated pie charts to show their distribution (Fig. 1). F1

Among gene categories, the largest group affected consists of transcripts with unknown function (expressed sequence tags; ESTs). Other transcripts encoded secreted factors and ligands, transport and binding proteins, and modifying enzymes. In summary, changes in expression profiles for these genes implicate *Pitx3* in some of the indirect controls upon morphogenesis such as those exerting an effect by means of regulation of secreted morphogens.

When assessed in broad strokes, the secreted factors and ligands are notably less up-regulated in morphants at stage 27 than at stage 19; however, by contrast, transcription factors are more up-regulated at stage 27. At stage 19, structural proteins were more profoundly affected (both up- or down-regulated) as a consequence of

Fig. 2. In situ hybridization analysis for putative targets of Pitx3 involved in eye development. Visual comparisons of gene expression patterns between right-side injected control-morpholino (Cmo) or *Pitx3*-morpholino (Pmo) embryos and their untreated contralateral control. **A–E**: *Pitx3* expression patterns are presented for comparison (adapted from Khosrowshahian et al., 2005; Smoczer et al., In Press). A: demonstrates faint but detectable signal throughout the ectoderm and in agreement with reverse transcriptase-polymerase chain reaction (RT-PCR) results. B: Expression is detectable throughout neural ridge, while at stage 22, the gene is expressed in a cleared specimen where an arrow indicates presomitic mesoderm. By stage 27 (D), *Pitx3* is detectable throughout much of the head ectoderm, as well as in branchial arches and somites. This pattern restricts later to somites, otic vesicle, lens, and brain (D). **F–G′**: *Vent2* expression is reduced in the developing eye field at stage 19 for the *Pitx3*-morpholino (Pmo) injected side (A′ white arrow) and at stage 27 (B′ black arrow), when compared with control-morpholino (Cmo) injected embryos (A,B). **H–I′**: *Pax6* shows reduced expression in eye field on Pmo side of embryos at stage 19 (C′ black arrow) and 27 (D′ white arrow). **J–J′**: *Crybb1* shows drastic loss of expression in the eye vesicle on the Pmo-treated side of stage 27 embryo (E′) and no difference caused by Cmo treatment (E). Dotted line represents the midline of the embryo, separating injected right side from contralateral left side control.

ID: manoharj | Black Lining: [ON] | Time: 21:04 | Path: N:/3b2/DVDY/Vol24109/120115/APPFile/JW-DVDY120115

TABLE 1. Data Summary for Genes Analyzed for Microarray Confirmation[a]

Gene ID	UniGene ID	Gene Highest BLASTn Hit (*Xenopus laevis*)	Microarray Ratio	Coincident	Pathway	Inductive	Secondary	RT-PCR Confirms	Change in ISH expression pattern	Putative BBE sites in 5kb of 5'UTR
Baz2b	Xl.19899	EST - Moderately similar to bromodomain adjacent to zinc finger domain, 2B	0.400 (19)	√		√	√	No	Yes	12
Bix4	Xl.399	homeobox protein BIX4 (bix4)	0.363 (27)		√			No	N/A	N/A
Crybb1	Xl.21502	Beta B1-crystallin (Crybb1)	0.325 (27)	√				Yes (27)	Yes	9
eFGF	Xl.1181	fibroblast growth factor 4B (fgf4-b) XeFGF(ii) embryonic fibroblast growth factor	0.406 (19)		√			No	N/A	4
Galectin IX	Xl.15089	EST - Fish-egg lectin-like isoform 1	0.154 (19) 0.246 (27)			√	√	No (19) Yes (27)	N/A	N/A
Gsc	Xl.801	Goosecoid (gsc)	2.328 (19) 4.743 (27)* 2.267 (27)*		√			No	N/A	14
Hes4 (Hairy 2b)	Xl.25977	basic-helix-loop-helix transcription factor hairy2b (hairy2)	0.299 (27)	√	√		√	Yes (27)	Yes (27)	14
Hes7[†] (Esr4)	Xl.15142	EST - Highly similar to *Xenopus laevis* Esr-4	0.381 (27)		√		√	No (27)	Yes	10
Hes7.1[†] (Xhr1)	Xl.12126	EST - Moderately similar to transcription factor HES-7.1-B (XHR1)	0.211 (27)	√	√			Yes	Yes	11
HoxA11	Xl.266	Homeobox A11 (HoxA11)	0.423 (27)		√			No	Yes	9
Lim1	Xl.21652	EST - LIM class homeodomain protein (Lim5/Lhx5) (lhx1)(Xlim-2B)	2.046 (27)		√		√	No	Yes	5
L-Maf	Xl.767	neural retina leucine zipper (nrl) bZIP transcription factor L-Maf (maf)	0.357 (19)	√				No	N/A	12
Obscnl	Xl.13958	EST - Weakly similar to obscurin, cytoskeletal calmodulin and titin-interacting RhoGEF	6.211 (19)	√				No (19)	Yes (27)	N/A

ID: manohari | Black Lining: [ON] | Time: 21:04 | Path: N:/3b2/DVDY/Vol24109/120115/APPFile/JW-DVDY120115

J_ID: Z7H Customer A_ID: DVDY23836 Cadmus Art: DVDY23836 Ed. Ref. No.: 12-0073 Date: 4-August-12 Stage: Page: 1490

TABLE 1. (Continued)

Gene ID	UniGene ID	Gene Highest BLASTn Hit (*Xenopus laevis*)	Microarray Ratio	Coincident	Pathway	Inductive	Secondary	RT-PCR Confirms	Change in ISH expression pattern	Putative BBE sites in 5kb of 5'UTR
Pax6	Xl.647	Paired box 6 (pax6-b)	0.226 (19) 0.477 (27)	√		√		No (19) Yes (27)	Yes	13
Rbp4l	Xl.17576	EST Weakly similar to RET_B Human plasma retinol-binding protein precursor (PRBP)	6.164 (19) 4.429 (27)	√				Yes	N/A	7
Rdh16	Xl.5553	EST - retinol dehydrogenase 16 (all-trans) (rdh16)	6.288 (19) 2.758 (27)	√		√		No	N/A	15
Ripply2	Xl.9206	Ledgerline (Stripy)	2.014 (19)	√	√		√	Yes (19)	Ambiguous	20
RXRa	Xl.877	retinoid X receptor, alpha (rxra)	0.319 (19)		√			No	N/A	1
Spr1	Xl.17379	Sp5 transcription factor (sp5) Sp1-like zinc-finger protein XSPR-1	0.441 (19)		√			No	Ambiguous	N/A
Spr2	Xl.2755.1	Sp1-like zinc-finger protein XSPR-2 GLI family zinc finger 1, gene 2 (gli1.2)	0.396 (27)		√			No	Yes	N/A
Vent2	Xl.37	VENT homeobox 2, gene 2 (ventx2.2; Xom)	0.406 (27)	√	√	√	√	Yes	Ambiguous	17
Wnt1	Xl.21471	Wnt1 related (Wnt7c)	0.274 (19) 0.172 (27)	N/A				N/A	N/A	8

[a]Combined in situ hybridization results with reverse transcriptase-polymerase chain reaction (RT-PCR) outcome, compared to the microarray prediction of gene transcript behavior in response to *xPitx3* knockdown. Highlighted genes represent the best-fit candidates for putative direct targets of Pitx3 since in situ hybridization and RT-PCR confirm the microarray data. Only the genes that had statistically significant RT-PCR results across three replicates were indicated on table as "Yes" confirmed by RT-PCR. For promoter analysis, putative Pitx3 and bicoid-binding elements (BBE) were searched in the 5000bp upstream region from ATG of *X. tropicalis* homologs where available at Ensembl.org (TAATCC, TAATCT, TAATGG, TAATCA, and putative binding sites for Pitx3; [Lebel et al., 2001]).

*Designate multiple Affymetrix probe sets that identify to the same gene transcript.

†Hes7 and Hes7.1 are discrete products arising from separate genes and that share only 40% amino acid identity. Hes7 shares 90% identity with murine Hes7.

J_ID: Z7H Customer A_ID: DVDY23836 Cadmus Art: DVDY23836 Ed. Ref. No.: 12-0073 Date: 4-August-12 Stage: Page: 1492

TABLE 2. Additional Genes Identified in the Microarray Data That Pertain to Genetic Pathways Implicated in this Study

Gene ID	UniGene ID	Gene Highest BLASTn Hit (*Xenopus laevis*)	Microarray ratio
Rax1	Xl.186	Retina and anterior neural fold homeobox (Rax-a)	2.148 (19)
βB3-crystallin	Xl.26355	Crystallin, beta B3 (crybb3)	0.366 (27)
γ-crystallin-like	Xl.23710	Transcribed locus, strongly similar to NP_001087320.1 crystallin, gamma A (*X. laevis*)	0.140 (19)
γB-crystallin	Xl.21441	Crystallin, gamma B (crygb)	0.298 (19)
βB3-crystallin-like	Xl.26349	69% similar to beta-crystallin B3 (*H. sapiens*)	3.800 (27)
Σ>βA4-crystallin	Xl.19126 (retired) replaced Xl.67080	Crystallin, beta 4 (cryba4)	0.223 (19) 2.741 (27)
βB1-crystallin-like	Xl.1337	Transcribed locus, strongly similar to XP_002938264.1 predicted: beta-crystallin B1-like (*X. tropicalis*)	2.122 (27)
Tbx4	Xl.21543	T-box 4 (tbx4)	0.436 (27)* 0.237 (27)*
Tbx5	Xl.529	T-box 5 (tbx5-b)	0.432 (27)
HoxA10	Xl.21639	Homeobox A10 (hoxa10)	0.373 (27)
HoxA13	Xl.21581	Homeobox A13 (hoxa13)	2.337 (27)
Galectin I	Xl.747	Lectin, galactoside-binding, soluble, 1 (lgals1)	2.264 (19) 0.436 (27)
Galectin IIa	Xl.17371	Galectin family xgalectin-IIa (xgalectin-IIa)	0.291 (19)
Galectin IIb	Xl.21879	Galectin 4 (lgals4-a)	2.367 (19)
Galectin IIIa	Xl.15364	Lectin, galactoside-binding, soluble, 9c (lgals9c-a)	0.414 (27)
Galectin IIIb	Xl.21878	Lectin, galactoside-binding, soluble, 9c (lgals9c-b)	0.304 (19)

Pitx3 knockdown than at stage 27. A similar picture developed for signal transduction. The disruptions are consistent with embryos experiencing impaired movement, signaling and morphological changes during neurulation at stage 19, when the body plan is arguably at its most ductile phase. Overall, chromatin modifying genes were up-regulated more than down-regulated at both stages.

Our aim was to use the microarray experiments to deduce novel *Pitx3* pathways, so we first focused upon the transcripts that were most up- and down-regulated in response to morpholino-mediated knockdown of *Pitx3*. In published studies involving samples from rapidly developing systems, microarray and RT-PCR results have occasionally been at odds. Moreover, microarrays are likely to be sensitive to subtle differences in the staging of developmental samples: quantitative data might not be fairly interpreted in absolute terms. We elected to categorize on the basis of trend: if gene expression levels were altered two-fold or more relative to controls, and this was repeated in a second experiment, we pursued the gene for further analysis using semi-quantitative RT-PCR analysis and riboprobe in situ hybridization. Genes that expressed in expression patterns that overlapped with *Pitx3* were deemed possible direct target genes of Pitx3. Of this subset, we focused upon those that also possessed putative Pitx3 binding motifs in the 5′ untranslated region (UTR) of *X. tropicalis* sequences. These were used for the reason that they were uniformly available, and all of the *Xenopus laevis* ESTs and genes that we have examined to date enjoy near perfect homology (Table 1). We then looked deeper into the data set to see if genes in the same signaling pathway or developmental process were similarly affected (Table 2). If the behaviors of the expanded set grouped in a logical manner, and if the behaviors were consistent with the *Pitx3* knockdown phenotypes, these genes were further analyzed by RT-PCR or in situ hybridization.

The affected genes can be classified as: potential direct targets of Pitx3; genes that operate within a *Pitx3* regulated pathway; or genes that are affected indirectly and outside of the domain of *Pitx3* expression as a result of grossly perturbed patterns of organ differentiation. Only four genes with putative Pitx3 binding motifs displayed both RT-PCR and riboprobe in situ hybridization patterns that were unequivocally consistent with the microarray trend: *Pax6*, *βb1Crystallin* (*Crybb1*), *Hes7.1*, and *Hes4*. Two others, *Vent2*, and *Ripply2* (aka *Ledgerline* or *Stripy*) displayed altered in situ hybridization patterns that were difficult to interpret with respect to expression level, because their respective patterns were affected differently in disparate domains (Table 1). For example, although *Vent2* expression is obliterated in the optic region consistent with the microarray trend, the gene is up-regulated in the posterior endoderm. Similarly, the banded pattern of *Ripply2* expression is anteriorized and delayed by morpholino at early stages, but appears to recover to some extent by stage 27.

In *X. laevis*, *Pitx3* expresses in the developing lens, the otic vesicle, and head mesenchyme, as well as in the branchial arches and along the anteroposterior axis in the developing somites (Pommereit et al., 2001; Khosrowshahian et al., 2005). Insofar as *Pitx3* is critical to lens placode function, it plays a critical role in frog retina induction (Khosrowshahian et al., 2005), so one might expect gene expression in retina to be indirectly affected as well. Eye pathway genes *Pax6*, *L-Maf*, and *Crybb1*, express in

ID: manoharj | Black Lining: [ON] | Time: 21:04 | Path: N:/3b2/DVDY/Vol24109/120115/APPFile/JW-DVDY120115

J_ID: Z7H Customer A_ID: DVDY23836 Cadmus Art: DVDY23836 Ed. Ref. No.: 12-0073 Date: 4-August-12 Stage: Page: 1493

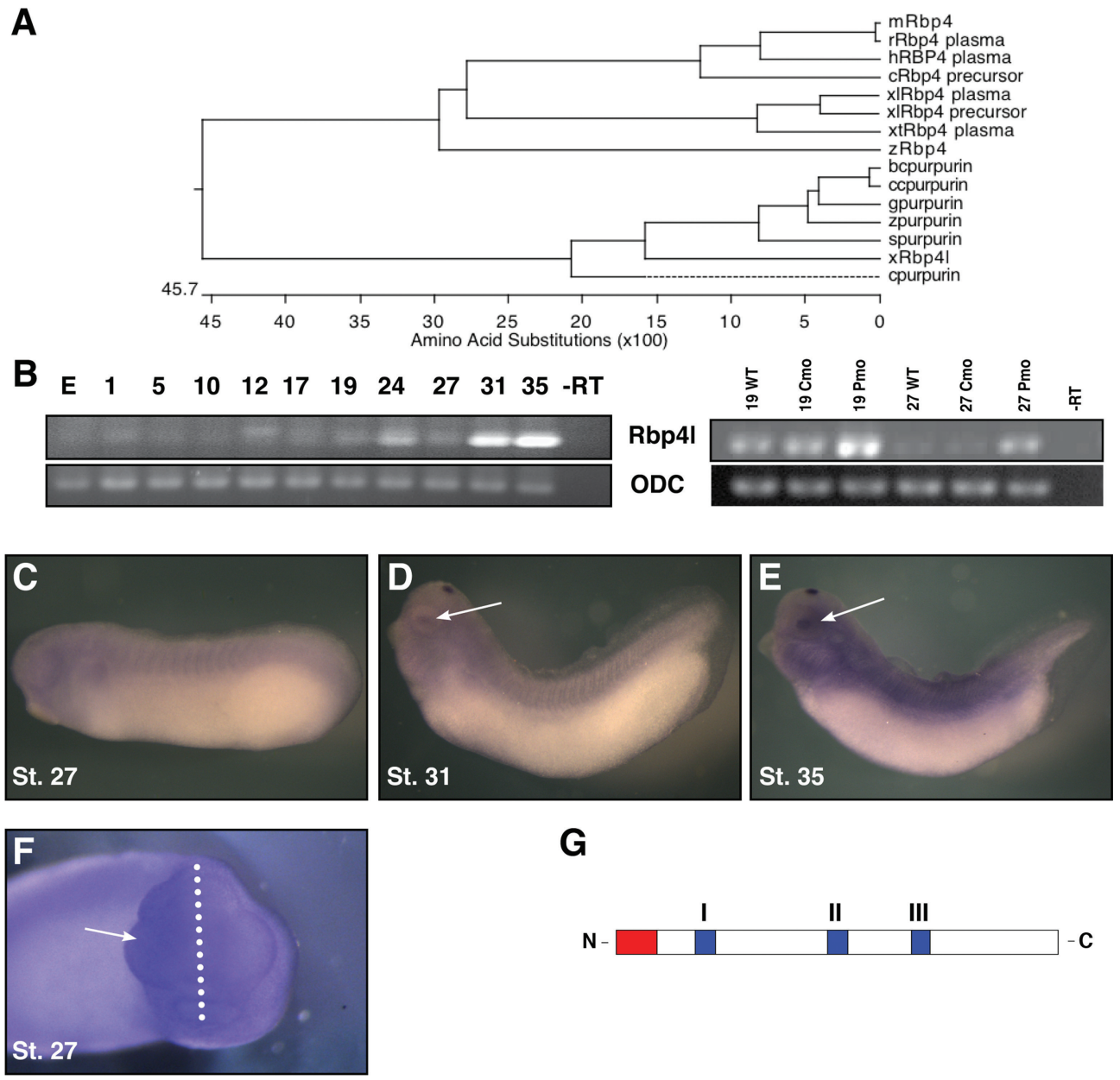

COLOR

Fig. 3. Characterization of a novel transcript, *Rbp4l*, in *X. laevis*. **A**: Protein alignment showing distinct groups between retinol binding proteins and purpurin family members. **B**: Temporal expression of *Rbp4l* throughout embryonic stages of development, showing slight detection at stages 17 and 24, and an increase in expression at stages 31 and 35. Confirmation of microarray predictions by means of reverse transcriptase-polymerase chain reaction (RT-PCR), showing an increase in *Rbp4l* expression in response to *Pitx3*-morpholino (Pmo) at stages 19 and 27, when compared with wild-type (WT) and control-morpholino (Cmo) treatments. **C**–**E**: In situ hybridization with antisense riboprobe against *Rbp4l* transcript shows expression at stages 27 (C), 31 (D), and 35 (E) concentrated in the developing lens (white arrows, D and E) and at the dorsal midline of the developing midbrain region. **F**: An embryo injected unilaterally with *Pitx3* morpholino on its right side (left of the dotted line) displayed enhanced and general expression in the craniofacial region. **G**: A schematic diagram of Rbp4l protein depicting a secretory signal at the N-terminus (red) and three characteristic lipocalin motifs (blue) that classify this protein as a member of the kernel subfamily of lipocalins. GenBank accession numbers used to generate phylogenetic tree (A) are as follows: xRbp4l CD362061 (*X. laevis*), rRbp4 plasma BC167099 (rat), mRbp4 BC031809 (mouse), hRBP4 plasma AL356214 (human), cRbp4 precursor NM_205238 (chick), xlRbp4 precursor NM_001087726 (*X. laevis*), xlRb4 plasma NM_001086998 (*X. laevis*), xtRbp4 plasma NM_001015748 (*X. tropicalis*), zRbp4 NM_130920 (zebrafish), zpurpurin AB242211 (zebrafish), spurpurin NP_001135080 (salmon), ccpurpurin NP_001187969 (channel catfish), gpurpurin BAD42450 (goldfish), bcpurpurin AD028302 (blue catfish), cpurpurin P08938 (chick).

the developing lens, and thus are good candidates for *Pitx3* targets. *Vent2*, *Rbp4l* (*purpurin*), *Galectin IX*, and *Rax1* express in early retina, and are all affected in morphants. They likely represent examples of the indirect consequences of *Pitx3* perturbation. Moreover, a microarray survey of *Aphakia* mice revealed a link between *Pitx3* perturbation and regulation of *Pax6* and *Rbp4* (Münster, 2005). All of the aforementioned

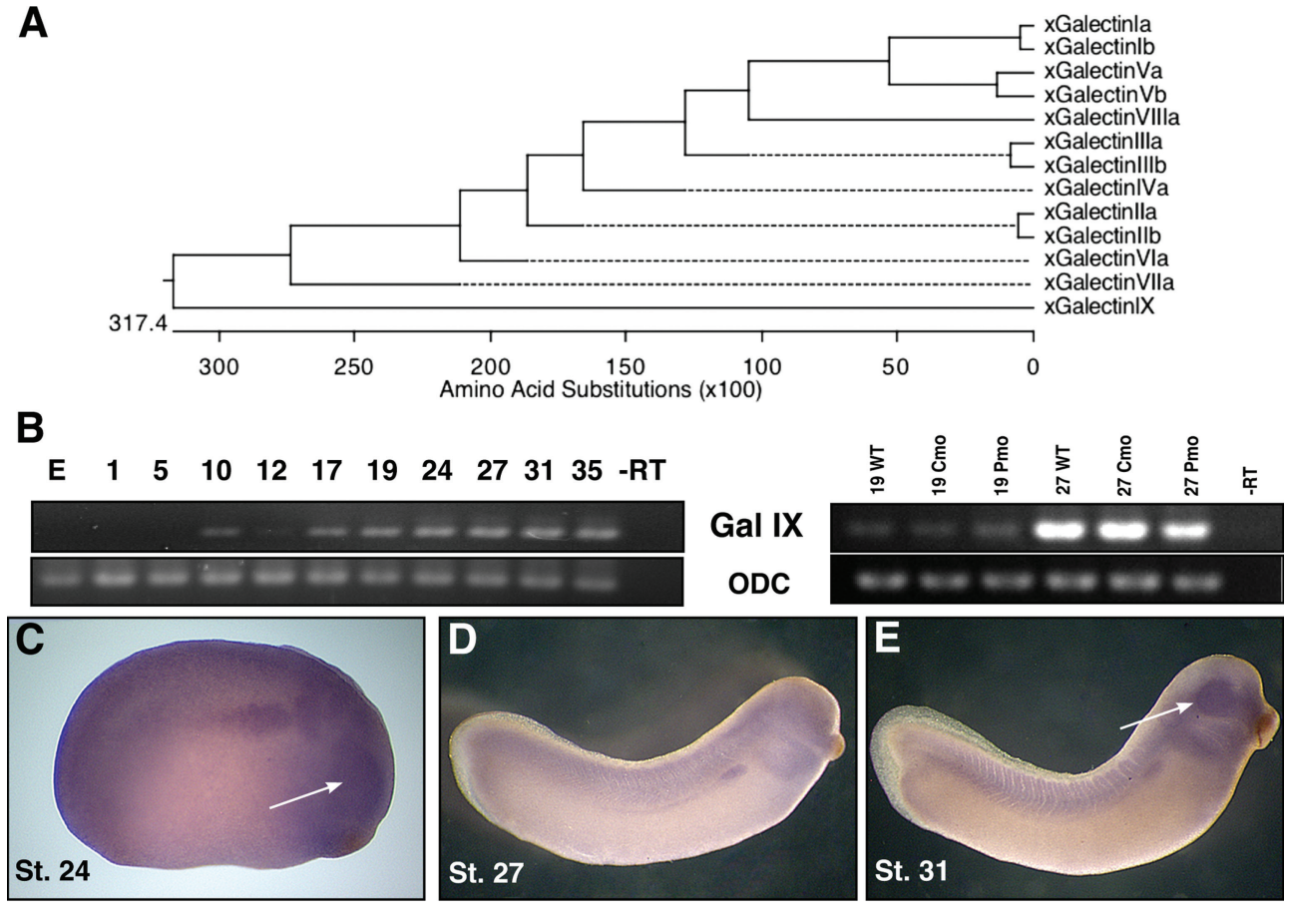

COLOR

Fig. 4.

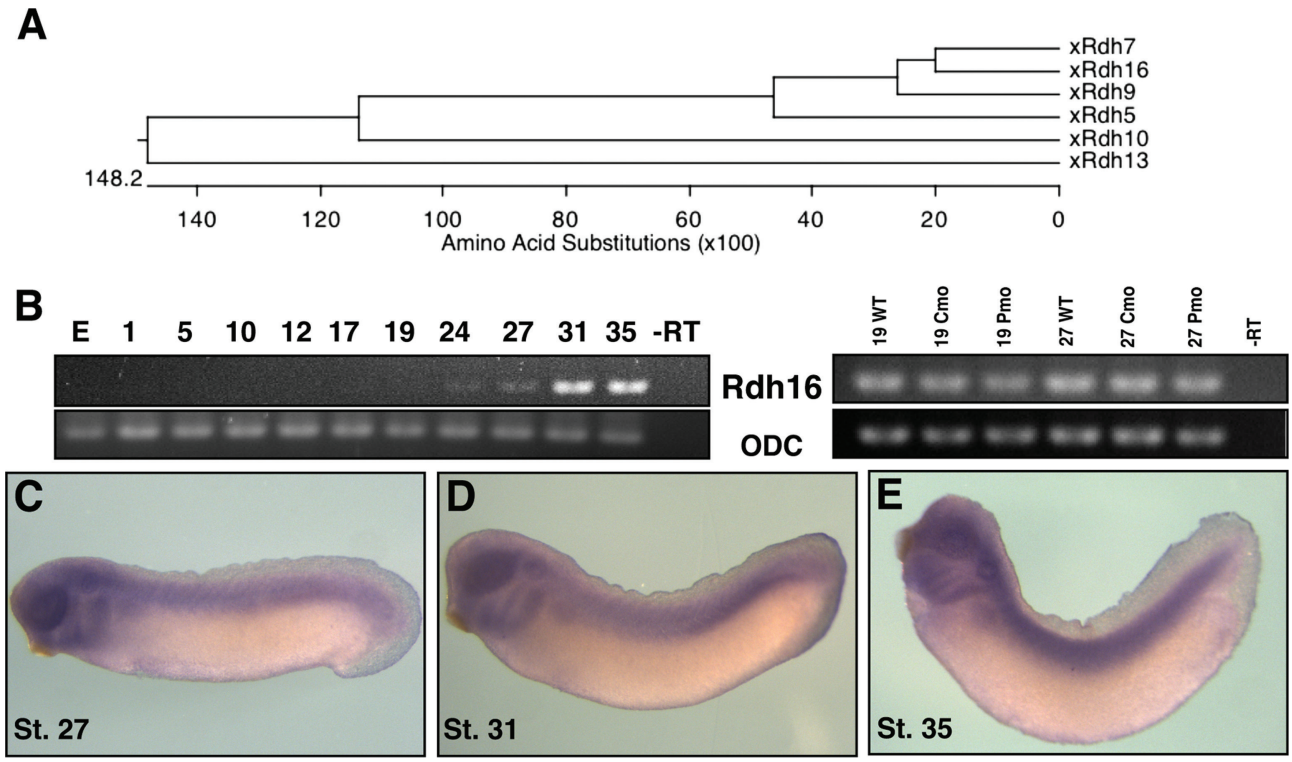

COLOR

Fig. 5.

J_ID: Z7H Customer A_ID: DVDY23836 Cadmus Art: DVDY23836 Ed. Ref. No.: 12-0073 Date: 4-August-12 Stage: Page: 1495

provide validation for the efficacy of the microarray. Unfortunately, none of the previously published and characterized targets of Pitx3 are represented on the microarray; however, one of the probe sets is to an EST that has homology to *MIP/Aquaporin O*, and it is down-regulated consistent with expectation.

Riboprobe In Situ Hybridization

We assessed the effect of *Pitx3* perturbation by injecting embryos at the two-cell stage such that the left and right sides of the developing embryo could be compared as embryogenesis ensued: morphant phenotypes were monitored on the "mutant" side relative to the contralateral control. Candidate gene expression patterns were assessed for perturbation in morphants and for a role in developing eye (Figs. 2–7), brain (Fig. 8), somite (Fig. 9), and tailbud (Fig. 10).

Eye development.

Among other domains, *Vent2* (a.k.a. *Ventx2*) is expressed in the dorsal retina (Fig. 2F,G) and it shows structural and functional homology to two *Drosophila* proteins, *Om1D* and *BarH1*, which are necessary for the differentiation of photoreceptor cells in the eye (Ladher et al., 1996). Along with *Vent2*, *Pax6*, and *Crybb1* are perturbed in *Pitx3* morphants (Fig. 2H–J).

Pax6 is required and sufficient for the initiation of eye development where it specifies the lens and retinal primordia (Halder et al., 1995), and it too is perturbed in our assays. The microarray and RT-PCR data regarding *L-Maf's* response to *Pitx3* perturbation was ambiguous but is nevertheless worth following up: its relationship to *Pitx3* has not been directly assessed; however, Maf binding sites are deleted in the promoter of a naturally occurring mouse *Pitx3* mutant (Semina et al., 2000) and *L-Maf* itself appears to reciprocally possesses 12 putative Pitx3 binding motifs in its 5′-UTR. *L-Maf* is expressed in the developing lens in response to inductive events from the optic vesicle, and it is directly targeted by Pax6 in chicks (Reza et al., 2002). *Maf* acts specifically in the lens fiber cells, where it can induce the expression of structural proteins such as the *γ*- and βb1-crystallins (Crybb1; Ishibashi and Yasuda, 2001; Cui et al., 2004). Given the presence of numerous potential Pitx3 binding sites in the *Crybb1* promoter, and the response of this gene in our *Pitx3* morphants, we speculate that Maf and Pitx3 act in tandem to activate the *Cry* genes. It is worth noting that other *Cry* genes represented on the microarray also underwent significant fractional change, albeit at less spectacular levels, namely: γ *crystallin* (0.14), γ *B crystallin* (0.3), β *B3 crystallin* (3.8), β *A3 crystallin* (2.74), and species weakly similar to human β *B1 crystallin* (2.12), and β *B3 crystallin* (0.37).

Novel* Xenopus *retinol-binding protein Rbp4l is expressed in lens. The microarray indicated that an EST sequence encoding a 197 amino acid protein (GenBank CD362061) was up-regulated at stages 19 and 27 by 6.2- and 4.4-fold, respectively. We obtained a clone from NIBB (XL060f11) and after sequencing it, we identified it as a member of the lipocalin protein family, namely *RBP4-like* (Retinoid binding protein 4 like -*Rbp4l*) or *purpurin*. These small extracellular proteins characteristically bind hydrophobic molecules and are typically known as transport proteins (Flower, 1996). Figure 3 shows that Rbp4l shares 73% residue identity with goldfish and salmon, 75% identity with zebrafish, and 78% similarity to chick Rbp4l. The similarity to human and murine retinoid-binding protein precursor is on 55 and 54%, respectively. Rbp4l consists of three conserved motifs that create a cup-shaped cavity, enabling the protein to bind retinol, and the protein possesses a signal peptide for secretion (Berman et al., 1987). In zebrafish, *rbp4l* is transcribed in photoreceptor cells, and the protein is diffusely detectable in all retinal layers (Tanaka et al., 2007). As a supplier of retinol, a precursor of retinoic acid, this protein activates the retinoic acid and retinoid receptor pathway (RAR and RXR, respectively; Nagy et al., 1996). Rbp4l functions as an extracellular matrix protein in the inter-photoreceptor matrix, and it appears to be necessary for cell adhesion and for the survival of photoreceptor cells in the neural retina (Berman et al., 1987; Nagy et al., 1996). Photoreceptor cells require retinol for phototransduction and retinol is carried to them from the pigmented retinal layer, through the matrix, bound to Rbp4l. In contrast,

Fig. 4. Characterization of a novel transcript *Galectin IX* in *X. laevis*. **A**: Protein alignment showing amino acid similarities between *Xenopus* Galectin family members. **B**: Temporal expression of *Galectin IX* throughout embryonic stages of development, shows expression beginning at gastrulation (stage 10), decreasing at stage 12, and expressing consistently at stages 17 through 35. Confirmation of microarray predictions by means of reverse transcriptase-polymerase chain reaction (RT-PCR), detect an increase in expression at stage 19 and a decrease at stage 27 for *Pitx3*-morpholino (Pmo) -treated samples, compared with wild-type (WT) and control-morpholino (Cmo). **C–E**: *Galectin IX* transcript expresses at stages 24 (C), 27 (D), and 31 (E) concentrated in the developing eye (white arrows) and presumptive pronephros, persisting in the nephric tubules and ducts. GenBank accession numbers used to generate phylogenetic tree (A) are as follows: xGalectinIa AB056478, xGalectinIb AB060969, xGalectinIIa AB060970, xGalectinIIb AB080016, xGalectinIIIa AB060971, xGalectinIIIb AB080017, xGalectinIVa AB060972, xGalectinVa M88105, xGalectinVb AB080018, xGalectinVIa AB080019, xGalectinVIIa AB080020, xGalectinVIIIa AB080021, xGalectinIX BJ056659.

Fig. 5. Characterization of a novel transcript, *Rdh16*, in *X. laevis*. **A**: Protein alignment showing amino acid similarities between *Xenopus* retinol dehydrogenase (rdh) family members. **B**: Temporal expression of *Rdh16* throughout embryonic stages of development shows faint expression beginning at stage 24 and 27, then increasing at stages 31 and 35. We were unable to confirm the microarray predictions by means of reverse transcriptase-polymerase chain reaction (RT-PCR), as no change in expression was detected between wild-type (WT) control-morpholino (Cmo), or *Pitx3*-morpholino (Pmo) embryos. **C–E**: In situ hybridization with antisense riboprobe against *Rdh16* transcript, shows expression at stages 27 (C), 31 (D), and 35 (E) concentrated in the eyecup, branchial arches, and otic vesicle, as well as along the lateral plate mesoderm, with a focus on the posterior half (D), and on in the developing myotomes. GenBank accession numbers used to generate phylogenetic tree (A) are as follows: xRdh16 NP_001083356, xRdh7 NP_001079189, xRdh13 NP_001085680, xRdh5 NP_001086194, xRdh9 NP_001090337, xRdh10 ACN32204.

ID: manoharj | Black Lining: [ON] | Time: 21:06 | Path: N:/3b2/DVDY/Vol24109/120115/APPFile/JW-DVDY120115

COLOR

Fig. 6.

COLOR

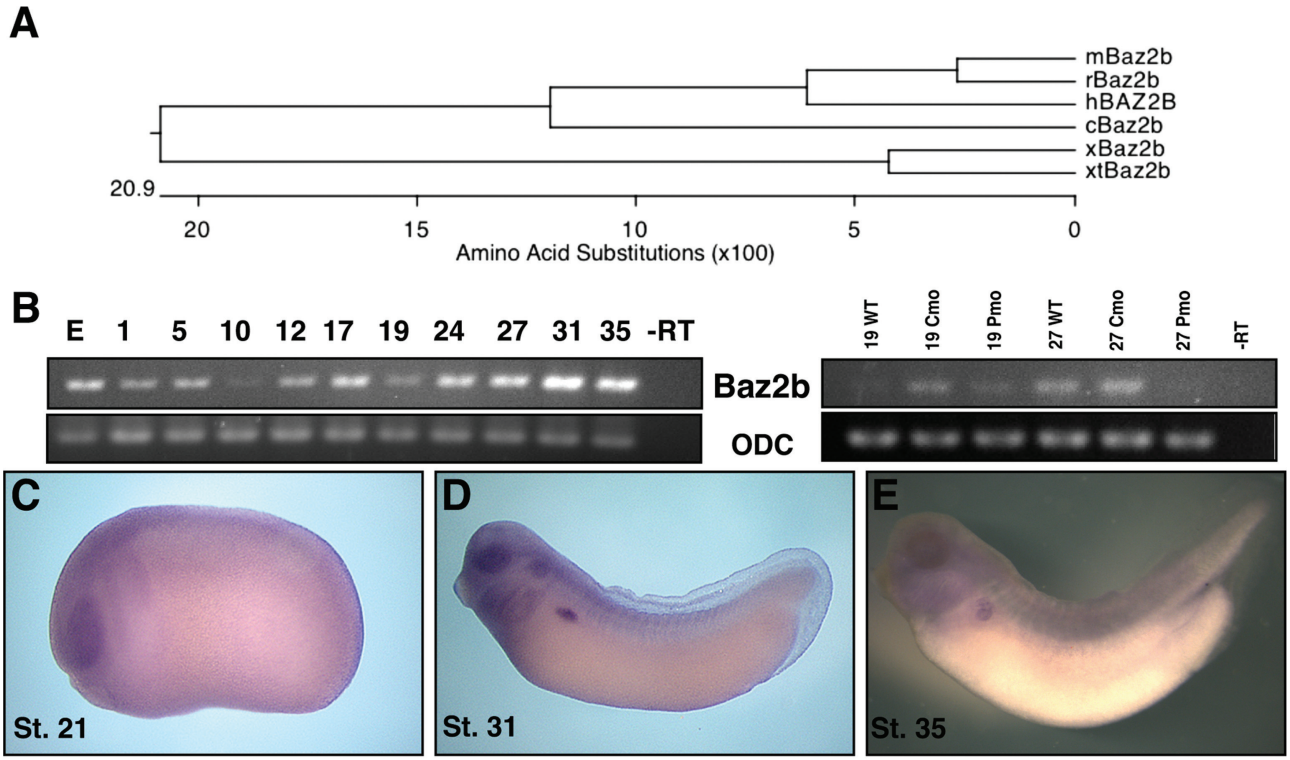

Fig. 7.

COLOR

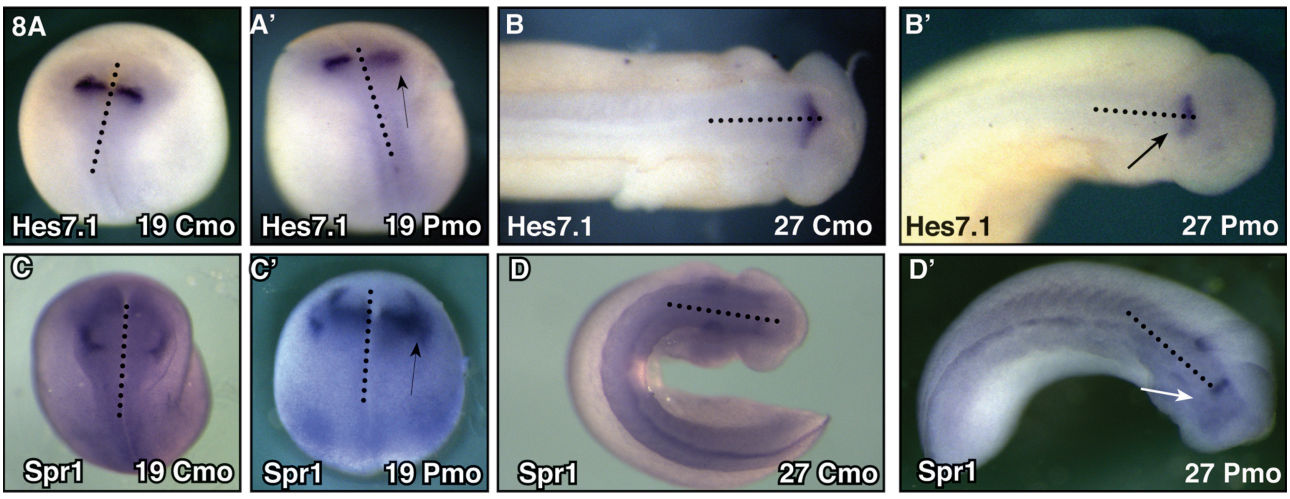

Fig. 8.

J_ID: Z7H Customer A_ID: DVDY23836 Cadmus Art: DVDY23836 Ed. Ref. No.: 12-0073 Date: 4-August-12 Stage: Page: 1497

the other RBPs, including Rbp4l's closest human homologue RBP4, are synthesized in the liver, bind to retinol in the blood (serum RBPs), and they transport retinol throughout the body to target cells (Goodman, 1981). Human *PITX3* maps to 10q25, and this is close to human *RBP4* and several retinoid synthetic *CYP* loci at 10q24 (Gray et al., 1997). According to the Ancora resource, the region near *Pitx3* is replete with highly conserved non-coding elements, so it is tempting to speculate that the genes are embedded within a conserved genome regulatory block (Kikuta et al., 2007; Engstrom et al., 2008).

Expression of *Rbp4l* is first detected by RT-PCR around stage 17 and increases past stage 35 (Fig. 3B). In situ hybridization shows that expression of this transcript concentrates in the lens area and as a pronounced spot along the midline on the top of the brain. It expresses at lower levels in the craniofacial region and somites (Fig. 3C–E). These expression patterns are distinct from those reported for *RBP4* and *purpurin*. RT-PCR analysis was performed and confirmed microarray trends: morphants demonstrated an increase in expression at stage 19 (1.84-fold) and 27 (2.88-fold; Fig. 3B). Consistent with the microarray and RT-PCR data, the gene undergoes up-regulation as a consequence of *Pitx3* knockdown (Fig. 3F). Because *Rbp4l* expression in *Pitx3* morphants is broadly up-regulated in the craniofacial region, our supposition is that *Pitx3* exerts its effects upon this gene earlier than the lens stage, and when *Pitx3* expression is more expansive. The murine homolog, *Rbp4*, is also affected by *Pitx3* depletion in *Aphakia* mutants (Münster, 2005). Taken together, the results for this novel retinol binding protein show the possibility of acting downstream of *Pitx3* in lens developmental pathways, where both genes are expressed.

Galectin IX *is expressed in eye field and retina.* One of the EST sequences from the microarray data identified mostly with the *Galectin* family, and represents a new family member (Fig. 4). We identify this sequence as a *Galectin IX* (GenBank accession no. JN975639). It is related to the tectonin family that encode beta-propeller repeats: the microarray reports a change in transcript levels at stage 19 (diminished to a fractional level of 0.15) and stage 27 (diminished to 0.25 of its former level). The function of a galectin can be extremely varied: it has intracellular and extracellular functions in cell adhesion, migration, proliferation, and apoptosis and that are stage- and tissue-specific (Cooper and Barondes, 1999).

Galectin IX, a gene uncharacterized with regard to expression patterns until this study, expresses in eye field and later in both lens and retina (Fig. 4). Little is known of its promoter structure, so it is early to speculate whether or not the gene is a direct target of Pitx3. In *Xenopus* alone, 12 different galectin proteins have been identified, numbered in order of discovery, and can be identified by means of galactose-binding ability and protein motifs, specifically carbohydrate recognition domains (Shoji et al., 2003). Other *Galectin* family members are expressed throughout the embryo in specific spatiotemporal patterns, suggesting varied developmental roles for each protein (Shoji et al., 2003). Additional *galectins* were identified in the microarray data: *Galectin IIb* (St.19 2.37-Fold), *Galectin I* (St.19 2.26-Fold, St.27 0.44-Fold), *Galectin IIIb* (St.19 0.30-Fold), *Galectin IIa* (St.19-0.29), *Galectin IIIa* (St.27-0.41). As a candidate Galectin, further functional assessment for galactose-binding affinity will be necessary to firmly classify this novel protein within the galectin family (Cooper and Barondes, 1999). Using an NIBB clone (XL103j23) we performed in situ hybridization to visualize the expression pattern of this novel transcript, which appears to be concentrated in the presumptive pronephros and eye regions (Fig. 4C–E). Expression begins at gastrulation, fades and then increases gradually beginning at neurulation (Fig. 4B). Curiously, RT-PCR for microarray confirmation (Fig. 3B) shows a fractional *increase* in expression at stage 19 (5.28), but the expected slight decrease at stage 27 (0.83) in morphants. This interaction is likely indirect because, even though expression patterns of *Pitx3* and *Galectin IX* overlap, in situ hybridizations do not demonstrate obvious changes of *Galectin IX* expression in morphants.

Fig. 6. In situ hybridization analysis for putative Pitx3 target genes *Obscnl* and *Baz2b*. Visual comparisons of gene expression patterns between control-morpholino (Cmo) and *Pitx3*-morpholino (Pmo) right side-injected embryos. **A**: *Obscnl* shows a loss of expression in the branchial arches (black arrow), otic vesicle, and retina when treated at stage 27 with Pmo (A′) versus Cmo (A). **B**: *Baz2b* is substantially reduced in response to Pmo (B′) in the retinal layer of the optic protuberance (white arrow), as well as in the pronephros and in the anterior region of the dorsal axis, when compared with Cmo (B).

Fig. 7. Characterization of a novel transcript, *Baz2b*, in *X. laevis*. **A**: Protein alignment showing amino acid similarities between *Baz2B* homologs across organisms. **B**: Temporal expression of *Baz2b* throughout embryonic stages of development show expression as a maternal transcript in the egg "E" and throughout development to tailbud stage, with slight reductions in transcript level at stages 10 and 19. B Confirmation of microarray predictions by means of reverse transcriptase-polymerase chain reaction (RT-PCR) show abolished expression at stage 27 in response to *Pitx3*-morpholino (Pmo) when compared with control-morpholino (Cmo) and wild-type (WT) embryos. **C–E**: *Baz2b* expression at stages 21 (C), 31 (D), and 35 (E) is concentrated in the developing eye, as well as the branchial arches and otic vesicle. Dark expression is seen in the pronephros, persisting in the tubules (E). **F**: A schematic diagram of Baz2b protein depicting various domains characteristic of Baz2B: methyl-CpG binding domain (MBD), DNA binding domain (DDT), zinc finger domain (Z), adjacent to the bromodomain (BR). GenBank accession numbers used to generate phylogenetic tree (A) are as follows: xBaz2b BQ400337 (*X. laevis*), mBaz2b BC150814 (mouse), rBaz2b NM_001108260 (rat), hBAZ2B NM_013450 (human), cBaz2b NM_204677 (chick), xtBaz2b BC166361 (*X. tropicalis*).

Fig. 8. In situ hybridization analysis for putative brain targets of Pitx3. Comparisons of gene expression patterns between right-side injected control-morpholino (Cmo) or *Pitx3*-morpholino (Pmo) embryos and their untreated contralateral control. **A–B′**: *Hes7.1* at stage 19 shows decreased expression in the midbrain hindbrain boundary or isthmus (black arrow) in response to Pmo (A′) versus Cmo (A) and again at stage 27 Pmo (B′) (black arrow) versus Cmo (B). **C–D′**: *Spr1* stained embryos show increased expression (black arrow) at stage 19 when treated with Pmo (C′), where no change in expression is observed with Cmo (C). At stage 27, *Spr1* expression in the isthmus is abolished on the Pmo side (D′) (white arrow). Dotted line represents the midline of the embryo, separating injected right-side from contralateral left-side control.

ID: manoharj | Black Lining: [ON] | Time: 21:07 | Path: N:/3b2/DVDY/Vol24109/120115/APPFile/JW-DVDY120115

J_ID: Z7H Customer A_ID: DVDY23836 Cadmus Art: DVDY23836 Ed. Ref. No.: 12-0073 Date: 4-August-12 Stage: Page: 1498

COLOR

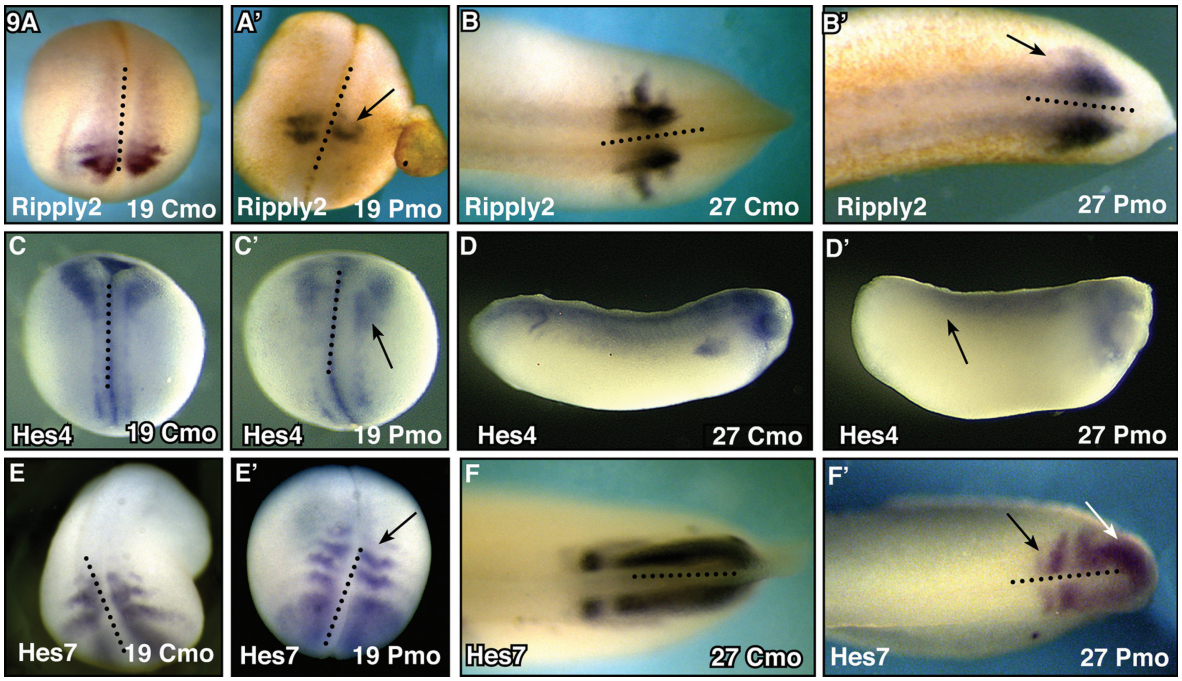

Fig. 9. In situ hybridization analysis for putative segmentation targets of Pitx3. Visual comparisons of gene expression patterns between right-side injected control-morpholino (Cmo) or *Pitx3*-morpholino (Pmo) embryos and contralateral control. **A**–**B**′: *Ripply2* expression, showing as two stripes in the presomitic mesoderm, shows an anterior shift (black arrow) in expression at stage 19 when treated with Pmo (A′) instead of Cmo (A). At stage 27, *Ripply2* expression pattern loses its distinct shape and becomes unrestricted in response to Pmo (B′), whereas with Cmo treatment, precise patterning of this gene expression remains intact (B). **C**–**D**′: *Hes4* expression becomes blurred in Pmo-treated embryos at stage 19 (C′) and at stage 27 (D′) *Hes4* expression is absent in the presomitic mesoderm (black arrow) and pronephros areas, compared with Cmo-treated embryos (D). **E**–**F**′: *Hes7* no longer expresses in the most anterior stripe (black arrow), and the remaining two stripes are shifted anteriorly in comparison to the contralateral control (E′). At stage 27, on the Pmo side of the embryo (F′), *Hes7* shows increased expression in the presomitic mesoderm (white arrow) and again an anterior shift of the striped pattern (black arrow). Dotted line represents the midline of the embryo, separating injected right-side from contralateral left-side control.

COLOR

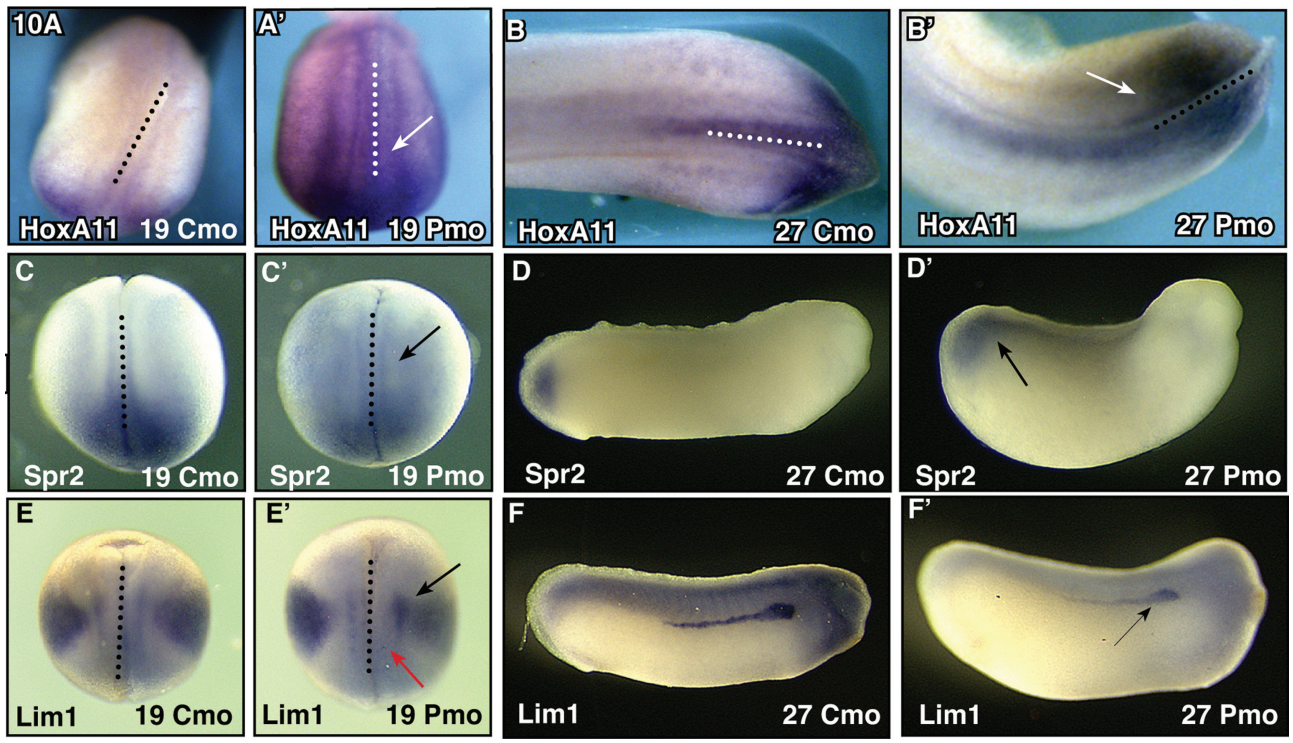

Fig. 10.

ID: manoharj | Black Lining: [ON] | Time: 21:07 | Path: N:/3b2/DVDY/Vol24109/120115/APPFile/JW-DVDY120115

J_ID: Z7H Customer A_ID: DVDY23836 Cadmus Art: DVDY23836 Ed. Ref. No.: 12-0073 Date: 4-August-12 Stage: Page: 1499

***Novel* Xenopus *Retinol Dehydrogenase* (Rdh16).** An EST sequence found in the microarray data can be identified as *retinol dehydrogenase 16* (*Rdh16*) (Fig. 5). Because retinoic acid is pertinent to many developmental processes, and Pitx3 has already been shown to regulate an aldehyde dehydrogenase, *AHD2* (Jacobs et al., 2007), this sequence is interesting as a putative downstream target of Pitx3. Retinol dehydrogenases are enzymes that catalyze the conversion of retinol (vitamin A) to retinal, an intermediate in the biosynthesis pathway of retinoic acid (Pares et al., 2008). These enzymes belong to the short-chain dehydrogenase/reductase (SDR) family. Their substrate is retinol bound to CRBP (cellular retinol binding protein) (Napoli et al., 1991) and they appear to be differentially expressed in different tissues (Chai et al., 1996). Their differential expression suggests tissue-specific roles for different family members. *Xenopus Rdh16* shows 51% similarity to human 11-cis *RDH*. The 11-cis RDH is synthesized in the retinal pigmented epithelium, is necessary for the generation of 11-cis retinaldehyde from retinol, and binds visual pigments in the eye (Wald, 1968; Simon et al., 1995, 1996). Microarray predicts a fold change of 6.288 at stage 19 and 2.758 at stage 27 for this transcript. We were unable to confirm this by RT-PCR (Fig. 5B) or in situ hybridization. We rule this gene out as a Pitx3 target.

The expression of this *retinol dehydrogenase* appears only in tailbud stages and is concentrated in the retinal layer of the developing retina, peripheral lens, otic vesicle, branchial arches, and along the anteroposterior axis in a gradient intensified at the posterior half (Fig. 5C–E). If this gene is a homolog of human 11-cis *RDH*, the expression in the eye would support a conserved functional role.

***Novel* Xenopus *Genes* Obscurin-Like *and Chromatin-Remodeling Protein* Baz2b.** Other genes may be indirect targets of *Pitx3* such as *obscurin-like* (*Obscnl*) in the eye field and branchial arches (Fig. 6A), and a chromatin remodeling gene *Baz2b* (Figs. 6B, 7). *Obscnl*, is an EST weakly similar to *obscurin, cytoskeletal calmodulin*, and titin-interacting *RhoGEF*. Because neither gene's expression pattern is altered in all *Pitx3*-expressing domains, it seems likely that they are affected by the morphological changes induced by *Pitx3* knockdown, and thus should be considered indirectly affected.

The EST with homology to the BAZ family of bromodomain-containing proteins (bromodomain adjacent to zinc finger) is tentatively assigned the designation *Xenopus Baz2b* (GenBank accession no. JN975638). The clone represents the 5′ half of a sequence encoding the N-terminus (921aa). This protein family contains a conserved bromodomain at the C-terminus, adjacent to a PHD zinc finger motif (Fig. 7F). Bromodomains, capable of binding acetyl-lysine residues, are often found in proteins with histone acetyltransferase (HAT) activity, and they are thought to play a role in chromatin-dependent gene regulation by unwinding histone-DNA complexes (Zeng and Zhou, 2002). Baz2b may have the ability to bind methylated CpG regions through a methyl-CpG binding domain (MBD; Fig. 4F). There is some evidence of BAZ proteins having the ability to interact with human homologs of ISWI, which in *Drosophila*, binds the BAZ1 protein homolog Acf1 to form the ACF chromatin remodeling complex (Ito et al., 1999; Jones et al., 2000a,b).

The microarray predicts that at stage 19 this transcript decreases in morphants to a fraction of 0.4 and at stage 27 to a fraction of 0.27. Unfortunately, by RT-PCR stage 19 transcript is *just* at the limit of detectability. RT-PCR shows expression throughout embryogenesis, beginning as a maternal transcript in the oocyte and persisting through tailbud stages, and confirms the microarray data by showing a drastic decrease in expression at stage 27 (to a fraction of 0.086), with undetected expression at stage 19 (Fig. 7B). Its spatial expression pattern, initially quite diffuse (not shown), condenses around the developing eye and pronephric structures during tailbud stages (Fig. 7C–E).

Since *Pitx3* has been shown to play major roles in both the lens and retina development, these genes correlate with a role for this transcription factor in specifying lens placode, initiating lens differentiation, and in inducing retina (Khosrowshahian et al., 2005).

Brain expression.

One candidate sequence was highly similar to *Hes-related 1*, and is tentatively re-assigned the name *Hes7.1* based upon homology to the *X. tropicalis* and human genes. This gene likely specifies the frog midbrain/hindbrain boundary, or isthmus (Shinga et al., 2001; Takada et al., 2005). The isthmus is an important organizer of brain regionalization and consequent patterning (Nakamura and Watanabe, 2005). When murine *Hes1* is disrupted, brain patterning mediated through the isthmus is damaged, and the mesencephalic dopaminergic (mDA) neurons fail to thrive. The same authors report that expression of both *Pitx3* and *tyrosine hydroxylase* is abnormal (Kameda et al., 2011). Because the related *Xenopus* homolog possesses 11 putative Pitx binding motifs, future studies should be sensitive to the possibility that *Hes1*/*Hes7.1* and *Pitx3* are engaged in a reciprocally regulatory relationship. *Spr1*, a *Xenopus laevis* transcription factor that is related to the human *Sp1* and mouse *Sp5* zinc finger genes, is expressed in the forebrain as well as the isthmus, where *eFGF* also plays a role (Isaacs et al., 1992; Ossipova et al., 2002). Both *Spr1* and *Hes7.1* show decreased expression in the isthmus in response to *Pitx3*-morpholino as assessed by in situ hybridization (Fig. 8).

Fig. 10. In situ hybridization analysis for putative tailbud targets of Pitx3. **A–B′**: *HoxA11* shows decreased posterior expression in the tailbud region (white arrows) of Pmo embryos at stages 19 (A′) and 27 (B′); **C–D′**: *Spr2* displays a broader and larger domain of expression (black arrows) when treated with Pmo, both at stage 19 (C′) and 27 (D′), compared with Cmo-treated embryos (C, D). **E–F′**: *Lim1* expression disappears from paraxial mesoderm (red arrow) and is up-regulated in lateral mesoderm (black arrow) at stage 19 when treated with Pmo (E′). At stage 27 (F′), Pmo reduces *Lim1* expression in the developing pronephros (black arrow) and in the head mesenchyme and along the dorsal axis.

ID: manoharj | Black Lining: [ON] | Time: 21:07 | Path: N:/3b2/DVDY/Vol24109/120115/APPFile/JW-DVDY120115

J_ID: Z7H Customer A_ID: DVDY23836 Cadmus Art: DVDY23836 Ed. Ref. No.: 12-0073 Date: 4-August-12 Stage: Page: 1500

Unfortunately, *tyrosine hydroxylase*, a gene critical to differentiation of dopaminergic neurons (mDA) of the *substantia nigra*, is not represented on the microarray. However, *Wnt1*, an early stage marker for murine isthmus (Würst et al., 1994), is both represented on the microarray and down-regulated (Table 2). Only an unworkably small fragment of the gene has been cloned in frog (Wolda and Moon, 1992). Because *Pitx3* is especially pertinent for the differentiation and maintenance of mDA neurons and because the isthmus is critical to development of the *substantia nigra* (Marchand and Poirier, 1983), it is tempting to speculate that this *Pitx3* effect is mediated through control of isthmus patterning at early developmental stages.

The expression patterns of *Lim1* will be discussed a greater length later, however, it is worth noting in the context of isthmus and *substantia nigra* (structures that are induced and patterned early by *Lim1* [Shawlot and Behringer, 1995]), that although the RT-PCR assays did not confirm the microarray data, nevertheless, in situ hybridization did. Moreover, *Lim1* possesses 5 evolutionarily conserved Pitx3 binding motifs. Based upon our preliminary slate of putative signaling partners, our suspicion is that *Pitx3* plays a heretofore uncharacterized role during gastrulation to pattern anterior-most structures—previous work has indicated that it expresses in fish hypoblast (Dutta et al., 2005), and somewhere in *Xenopus* pregastrula (RT-PCR, uncharacterized and low-expression location; Khosrowshahian et al., 2005).

Segmentation and tailbud signaling.

The *Ripply* family, *Ripply1* (*bowline*), *Ripply2* (*ledgerline*, *stripy*) and *Ripply3* serve as transcriptional repressors that are necessary for proper boundary formation during somitogenesis. The *Ripply* genes appear to act by balancing the FGF/RA signaling wave front and thereby regulate the emergence of new somites: this regulation is likely mediated by interaction with *T-box* genes (Chan et al., 2006; Kawamura et al., 2008; Hitachi et al., 2009). It is interesting that both *Tbx4* and *Tbx5* go down in our data set (0.237 and 0.436 for each of the two *Tbx4* probands, and 0.432 for *Tbx5*). *Ripply2*, *Hes4*, and *Hes7* are perturbed in *Pitx3* morphants (Fig. 9), and *Ripply2* possesses 20 Pitx3 binding sites in its 5′-UTR. *Hes7* expression patterns confirmed the microarray data, however, triplicate RT-PCR reactions did not substantiate this statistically. We note that RT-PCR consistency has historically been a problem in microarray studies (Altmann et al., 2001; Buchtova et al., 2010), and given the presence of 10 Pitx3 binding motifs within the 5′-UTR of *Hes7*, we are inclined to pursue this gene's candidacy further. Perturbation of *Hes4* is complex: it appears to up-regulate at early stages, to remain unchanged through neurulation, but to be inhibited at tailbud stages (Smoczer et al., In Press). *Hes4* and *Hes7* are factors that function downstream of the *Notch* pathway during somitogenesis and that mediate segmental patterning of the presomitic mesoderm where they serve as components of the segmentation clock (Jen et al., 1999; Tsuji et al., 2003; Murato et al., 2007). Recently, presomitic expression has been reported for *Pitx3* and its perturbation results in anomalous segmentation presenting as a bent dorsal axis and aberrant somite morphogenesis (Smoczer et al., In Press). *Ripply2* morphants also produce bent dorsal axes and shift *Hes4* and *Hes7* expression patterns anteriorly (Chan et al., 2006). Further research is necessary to deduce which of these are direct downstream targets of *Pitx3*, but a good starting point would be to test if Pitx3 modulates *Ripply2* and thereby indirectly alters expression of the *Hes* genes.

Both *eFGF* and *RXR*α are transcribed in the tailbud and thus may be factors that are affected by *Ripply2* (Chan et al., 2006). *eFGF* extends to the posterior of the body axis and into the proliferating tailbud where notochord and somites continue to emerge. *eFGF* is also expressed later in the myotome of the trunk (Isaacs et al., 1992). Both *eFGF* and *RXR*α appear regulated by Pitx3 in the microarray dataset, but neither confirm by RT-PCR. The expression levels are too low to be reliably detected by in situ hybridization at stage 19 and 27; however, both possess consensus Pitx3 binding motifs in their respective 5′-UTR. Given the effects of *Pitx3* perturbation upon the somitogenesis- and tailbud-expressing genes *HoxA11*, *Spr2*, and *Lim1* (Fig. 10), it might be worth re-examining their failed candidacy as targets.

Spr2 and *HoxA11* are affected by *Pitx3* mis-regulation (Fig. 10). *HoxA11* specifies positional identity along the anteroposterior axis and is largely expressed in the posterior notochord and tailbud mesoderm (Lombardo and Slack, 2001). Other *Hox* genes are affected to a lesser, though still significant fractional degree: *HoxA13* (2.4), and *HoxA10* (0.37). The differential effect upon these genes renders an indirect mediation by retinoid metabolism unlikely. *Lim1* expression undergoes a complex modulation of expression: lateral mesoderm expression increases, while in paraxial mesoderm, expression is abolished. *Spr2* and *Vent2* are expressed in the developing tailbud (Ladher et al., 1996; Ossipova et al., 2002), so effects in this domain would also be reflected in the microarray.

Indirectly characterized early perturbation effects.

Although the microarray data was analyzed for embryos at stages 19 and 27, a significant number of candidates are pertinent for early patterning of the embryo, and moreover, are known to interact with each other in a manner consistent with Pitx3 impinging upon their respective regulatory networks. *Pitx3* has been detected at early stages in the embryo (stage 8; Khosrowshahian et al., 2005) suggesting an unknown function for this transcription factor at earlier stages. One of our candidate targets, *Vent2*, provides ventralizing information and perhaps signals for the differentiation of the epidermis (Ladher et al., 1996). This factor directly down-regulates the homeobox gene *Goosecoid* (*Gsc*), which is expressed in Spemann's organizer and then becomes undetectable as the embryo undergoes neurulation (Cho et al., 1991; Trindade et al., 1999). *Gsc* is responsible for the development of dorsal structures (Cho et al., 1991). These two genes, *Vent-2*

ID: manoharj | Black Lining: [ON] | Time: 21:07 | Path: N:/3b2/DVDY/Vol24109/120115/APPFile/JW-DVDY120115

J_ID: Z7H Customer A_ID: DVDY23836 Cadmus Art: DVDY23836 Ed. Ref. No.: 12-0073 Date: 4-August-12 Stage: Page: 1501

TABLE 3. Parameters and Primer Sequences Used in RT-PCR Experiments

Gene	Primers	Size	Anneal temp	GenBank no.	Reference
ODC	Sense: 5′ - GTC AAT GAT GGA GTG TAT G - 3′ Antisense: 5′ - TCC ATT CCG CTC TCC TGA - 3′	385bp	57°C		XenBase
Lim1	Sense: 5′ - CCG ACA CAT AAG GGA GCA GC - 3′ Antisense: 5′ - CTG GTG GGT GTG ACA AAT GG - 3′	573bp	60°C	X63889	Homemade
Spr1	Sense: 5′ - CCA GGT ACA AGT CCT ACT GA - 3′ Antisense: 5′ - GAG TGC CAC CTC AAA TGA GC - 3′	752bp	54°C	AY062264	Ossipova et al., 2002
Spr2	Sense: 5′ - CAA ACT GTT GCC TCT CAT GAG - 3′ Antisense: 5′ - CAC TTA CAC CTC CGG CAG CGC - 3′	380bp	54°C	AY062263	Ossipova et al., 2002
Vent2	Sense: 5′ - GCT TTC TCC TCG GTT GAA TG - 3′ Antisense: 5′ - TCT CCT TCA GGG GCT GTA GA - 3′	461bp	57°C	X98454	Homemade
Hes4	Sense: 5′ - GCA CGA ACG AAG TCA CAC GA - 3′ Antisense: 5′ - GCT GGG TTG GGA ATG AGG AAA G - 3′	297bp	65°C	AF139914	Homemade
Hes7.1	Sense: 5′- TGT AAT GTG CTC AAA TGG CG - 3′ Antisense: 5′ - TCC GTC AGC CCT ACA AAG AC – 3′	336bp	54°C	BJ088128	Homemade
Obscnl	Sense: 5’ – ACA GTA TGG TTC ACA GCC – 3’ Antisense: 5’ – CAG TTG GCA CAT CAA TCC AG – 3’	283bp	57°C	BJ085487	Homemade
Gsc	Sense: 5′ - ACA ACT GGA AGC ACT GGA - 3′ Antisense: 5′ - TCT TAT TCC AGA GGA ACC - 3′	279bp	52°C	M81481	XenBase
RXRα	Sense: 5′ - AAG ATA CTT GAG GCG GAG CA - 3′ Antisense: 5′ - TTC GGG GTA TTT CTG TTT GC - 3′	531bp	54°C	L11446	Homemade
L-Maf	Sense: 5′ - CTT GCT CCT CCT CAA TCT CTG G - 3′ Antisense: 5′ -CCG ACA AAG GCG AAA GCT GGT G - 3′	331bp	54°C	AF202059	Ishibashi and Yasuda, 2001
eFGF	Sense: 5′ - TTA CCG GAC GGA AGG ATA - 3′ Antisense: 5′ - CCT CGA TTC GTA AGC GTT - 3′	222bp	56°C	X62594	Kroll Lab
Bix4	Sense: 5′ - CAG AAC AGG AGA TCA AAA GC - 3′ Antisense: 5′ - CGG GTA GGT ACT AGA TGC TG – 3’	414bp	54°C	AF079562	Homemade
Hes7	Sense: 5’ – TGT TGG CTT GAA AGG TTT GT - 3′ Antisense: 5’ – CTC AAA ATG TGT CAT AAT CCA - 3′	394bp	60°C	BJ058661	Homemade
Ripply2	Sense: 5’ – ATG GAG CCG AAT CAA CAG C - 3′ Antisense: 5’ – TGT CTT CCT CTT CAG AGT CA - 3′	352bp	57°C	AB073615	Homemade
Crybb1	Sense: 5’ – CGT GGT GAG ATG TTT ATC CTG GAG - 3′ Antisense: 5’ – CCT TCT GGT GCC ATT GAT TGT CTC - 3′	394bp	60°C	CD303346	Homemade
Pax6	Sense: 5’ – GCA ACC TGG CGA GCG ATA AGC - 3′ Antisense: 5’ –CCT GCC GTC TCT GGT TCC GTA GTT - 3′	448bp	56°C	U77532	Zuber et al., 2003
HoxA11	Sense: 5’ – AAT CCC TCC AAT GTC TAC CAC C - 3′ Antisense: 5’ – CTG GTA TTT GGT ATA CGG GCA C – 3’	363bp	56°C	AJ319668	Slack et al., 2001
Rbp4l	Sense: 5’ – AGA TGC AAT GCT CAG TCC T – 3’ Antisense: 5’ – GCG GGA GAA TAT AAT AGA ATA – 3’	432bp	54°C	CD362061	Homemade
GalectinIX	Sense: 5’ – CCC GTG CCT GGT ATT TCA – 3’ Antisense: 5’ – ACC TGG CTG GAG TGA ACA – 3’	448bp	55°C	BJ056659	Homemade
Baz2b	Sense: 5’ – AAG ATG ATG ATG AGG ACG A – 3’ Antisense: 5’ – CCA TTT TAG CCT GCT GTT TC – 3’	837bp	55°C	BQ400337	Homemade
Rdh16	Sense: 5’ – CTG CGA CTC TGG GTT TGG A – 3’ Antisense: 5’ – TCA TAG CCG GCA GAG TAG – 3’	750bp	57°C	BG514525	Homemade

and *Gsc*, play antagonistic roles in the establishment of the dorsoventral axis. *Lim1* expression peaks at gastrulation in Spemann's organizer, and has the ability to directly activate *Gsc* and maintain its expression in the prechordal plate (Mochizuki et al., 2000). All three are represented as Pitx3-sensitive in the microarray; however, *Gsc* expresses too early to have been monitored in our riboprobe in situ hybridization although it should be noted that *Gsc* possesses 14 Pitx3 motifs in its 5′-UTR.

Bix4 is a *Brachyury*-inducible homeobox-containing gene and is thought to induce both mesoderm and endoderm formation depending on the concentration of its encoded protein (Tada et al., 1998). It expresses earlier than we monitored by in situ hybridization at stages 19 or 27. Similarly, *eFGF* and *RXR*α are also expressed early in development, well before the stages that we assessed. *eFGF* is most similar to *FGF-6* and *FGF-4* in mammals, yet may represent a novel FGF secreted factor that has both mesoderm-inducing properties and roles in anteroposterior patterning (Isaacs et al., 1994). *RXR*α encodes a retinoid X receptor that is part of the nuclear receptor family that mediates the effects of retinoic acid upon embryos. Expression of *RXR*α begins as a maternal transcript in the oocyte, and then is temporarily abolished before gastrulation, leading to a role for this receptor in early patterning of the embryo (Blumberg et al., 1992). RA provides positional information and helps to pattern the

ID: manoharj | Black Lining: [ON] | Time: 21:07 | Path: N:/3b2/DVDY/Vol24109/120115/APPFile/JW-DVDY120115

J_ID: Z7H Customer A_ID: DVDY23836 Cadmus Art: DVDY23836 Ed. Ref. No.: 12-0073 Date: 4-August-12 Stage: Page: 1502

TABLE 4. Gene-Specific Information Regarding Restriction Enzymes and RNA Polymerases Used to Generate Riboprobes for In Situ Hybridization Experiments

Gene	Plasmid	Restriction enzyme	RNA Polymerase	Reference/source
Lim1	pBSKS+/Xlim-1 (pXH32)	*Xho*I	T7	Dawid, I. (NICHD)
Vent2	pBS-XOM	*Eco*RI	T7	Ladher et al., 1996
Spr1	pBSTSp1 T3/597(2-3)-2/XSPR-1	*Not*I	T3	Ossipova et al., 2002
Spr2	pCS2+NLSmyc/XSPR-2	*Xho*I	T7	Ossipova, O. (unpublished)
Hes4	XL409i23ex	*Eco*RI	T7	NIBB
Rbp4l	XL060f11	*Bam*HI	T7	NIBB
GalectinIX	XL103j23	*Eco*RI	T7	NIBB
Baz2b	6989392	*Sal*I	T7	I.M.A.G.E.
Rdh16	9897030	*Sal*I	T7	I.M.A.G.E
Hes7.1	XL091p04	*Eco*RI	T7	NIBB
Obscnl	XL106a24	*Eco*RI	T7	NIBB
Hes7	XL060b05	*Eco*RI	T7	NIBB
Ripply2	pCS/ledgerline	*Cla*I	T7	Asashima M. lab
Crybb1		*Hin*dIII	T7	Henry J. lab
Pax6		*Eco*RI	SP6	Lupo G. lab
HoxA11	pGMT/HoxA11	*Not*I	T7	Slack et al., 2001

anteroposterior body axis, mostly by mediating posterior transformation of the embryo (Durston et al., 1989).

Conclusion

Microarray analysis is a useful tool to monitor the influence of a gene upon the entire transcriptome of an organism. However, the generated data set is quite elaborate and deducing pertinent trends can be a challenging process. The information represented in this study provides a global view of general developmental processes in which *Pitx3* may be involved. New genetic players have been identified as putative *Pitx3* targets in the already established eye and brain developmental processes. In addition, based on genes identified by the microarray, novel roles for *Pitx3* can be inferred for regulation of early patterning events and the development of the anterior–posterior body axis.

EXPERIMENTAL PROCEDURES

Embryo Collection and Manipulation

Staging, de-jellying, and culturing of *Xenopus laevis* embryos were conducted as previously described (Nieuwkoop and Faber, 1967; Drysdale and Elinson, 1991). Animals were reared and used in accordance with University, Provincial, and Federal regulations. Fluorescently labeled morpholinos for either control or experimental *Pitx3* treatments were injected as previously described (Khosrowshahian et al., 2005; Smoczer et al., In Press). Essentially, 4.6-nl injections were made into the animal pole of embryos at the 1-cell stages for RNA collection and one- or two-cell stages for in situ hybridization. Injected embryos were cultured in 0.3 × MBS and 2% Ficoll-400 (Sigma) at 17°C for at least 1 hr to allow healing before being removed and allowed to develop at 12°C in 0.1 × MBS.

RNA Preparation and Microarray Analysis

At staged intervals, embryos were removed for RNA isolation, lysed, and processed in Trizol as per manufacturer's instructions (Invitrogen). We then used DNAseI to remove genomic DNA, and ran the product over Qiagen RNeasy columns for purification. RNA quality was assessed using the Agilent 2100 Bioanalyzer (Agilent Technologies Inc., Palo Alto, CA) and the RNA 6000 Nano kit (Caliper Life Sciences, Mountain View, CA).

All GeneChips were processed from two biological replicates at the London Regional Genomics Centre (Robarts Research Institute, London, Ontario, Canada; http://www.lrgc.ca). Biotinylated complimentary RNA (cRNA) was prepared from 10 μg of total RNA as per the Affymetrix GeneChip Technical Analysis Manual (Affymetrix, Santa Clara, CA). Double-stranded cDNA was synthesized using SuperScriptII (Invitrogen, Carlsbad, CA) and oligo$(dT)_{24}$ primers. Biotin-labeled cRNA was prepared by cDNA in vitro transcription using the BioArray High-Yield RNA Transcript Labeling kit (Enzo Biochem, New York) incorporating biotinylated UTP and CTP. A total of 15 μg of labeled cRNA was hybridized to *Xenopus laevis* GeneChips for 16 hr at 45°C as described in the Affymetrix Technical Analysis Manual (Affymetrix). GeneChips were stained with Streptavidin-Phycoerythrin, followed by an antibody solution and a second Streptavidin-Phycoerythrin solution, with all liquid handling performed by a GeneChip Fluidics Station 400. GeneChips were scanned with the Affymetrix GeneChip Scanner 3000 (Affymetrix).

Signal intensities for genes were generated using GCOS1.2 (Affymetrix) using default values for the Statistical Expression algorithm parameters and a Target Signal of 150 for all probe sets and a Normalization Value of 1. Normalization was performed in GeneSpring 7.2 (Agilent Technologies Inc., Palo Alto, CA). Data were first transformed (measurements less than 0.01 set to 0.01) and then normalized per chip to the 50th percentile, and per gene to control samples for each stage. We performed two biological replicates and filtered the data based upon fold change with a cut off P value set at 0.05.

ID: manoharj | Black Lining: [ON] | Time: 21:07 | Path: N:/3b2/DVDY/Vol24109/120115/APPFile/JW-DVDY120115

J_ID: Z7H Customer A_ID: DVDY23836 Cadmus Art: DVDY23836 Ed. Ref. No.: 12-0073 Date: 4-August-12 Stage: Page: 1503

RT-PCR

cDNA was made using Omniscript reverse transcriptase (Qiagen) and Oligo$(dT)_{18}$ primers (Sigma) from 1ug total RNA for microarray confirmation and from 10uL mRNA further isolated (GenElute Direct mRNA Miniprep Kit; Sigma) for stage analysis of novel EST sequences. RT-PCR was performed at various annealing temperatures and cycle numbers, resulting in five time-points that were ultimately graphed. A cycle at the linear phase of amplification was selected for each gene and standardized against ODC. Fold change for microarray confirmation was determined by comparing gene amplification of control-morpholino-treated samples with *Pitx3*-morpholino-treated samples. Primers and parameters are outline in Table 3.

Whole-Mount In Situ Hybridization

In situ hybridizations were performed according to established protocols (Harland, 1991) using digoxygenin-labeled riboprobes. We probed genes that were either two times up- or down-regulated as a consequence of *Pitx3*-morpholino perturbation, deemed by the microarray analysis. The probes used were generated from plasmids that were either the generous gifts of colleagues, the NIBB/NIG/NBRP *Xenopus laevis* EST project, or were purchased from ATCC (see Tables). When a probe revealed a temporal and spatial expression pattern that overlapped with the known activity of *Pitx3*, further in situ hybridizations were conducted on specimens that had been unilaterally injected with morpholino (control- or *Pitx3*-morpholino) at the two-cell stage: expression on the perturbed side could be compared with the contralateral control, and the trend predicted by the microarray thereby confirmed. Probes were prepared from vectors as outlined in Table 4.

Identification of Novel Genes

Some of the most differentially expressed but previously uncharacterized EST sequences were explored. Their spatial expression pattern was visualized by means of in situ hybridization and the temporal expression pattern was then investigated using RT-PCR throughout embryonic stages of development. Varied stages were used to determine specific developmental events: unfertilized egg (E) and stage 5 for maternal transcripts, stage 10 (early gastrula), stage 12 (neural anlage), stage 17 (onset of somitogenesis), stage 19 (neural tube), stage 24 (tailbud), stage 27 (lens differentiation), stage 31 (cardiac looping), stage 35 (blood supply; Nieuwkoop and Faber, 1967). Phylogenic profiles and functional attributes were deduced using Blastp searches within GenBank and homolog alignments using the Megalign program of DNASTAR Lasergene 7.2.

ACKNOWLEDGMENTS

The authors thank the numerous colleagues who provided us with probes, and particularly to Dr. Kitayama and Dr. Ueno, at the NIBB, without whose patient, generous, and numerous gifts this work could not have proceeded. Thanks also to David Carter of the London Regional Genomics Center, Robarts Research Institute, London, Ontario. M.J.C. was funded by the Natural Sciences and Engineering Research Council (NSERC) of Canada. F.K.S. was supported by an NSERC PGS, and M.W. was partially supported by an Ontario Graduate Scholarship.

REFERENCES

Altmann CR, Bell E, Sczyrba A, Pun J, Bekiranov S, Gaasterland T, Brivanlou AH. 2001. Microarray-based analysis of early development in Xenopus laevis. Dev Biol 236:64–75.

Amendt BA, Sutherland LB, Semina EV, Russo AF. 1998. The molecular basis of Rieger syndrome. Analysis of Pitx2 homeodomain protein activities. J Biol Chem 273:20066–20072.

Berman P, Gray P, Chen E, Keyser K, Ehrlich D, Karten H, LaCorbiere M, Esch F, Schubert D. 1987. Sequence analysis, cellular localization, and expression of a neuroretina adhesion and cell survival molecule. Cell 51:135–142.

Blumberg B, Mangelsdorf DJ, Dyck JA, Bittner DA, Evans RM, De Robertis EM. 1992. Multiple retinoid-responsive receptors in a single cell: families of retinoid "X" receptors in the Xenopus egg. Proc Natl Acad Sci U S A 89: 2321–2325.

Buchtova M, Kuo WP, Nimmagadda S, Benson SL, Geetha-Loganathan P, Logan C, Au-Yeung T, Chiang E, Fu K, Richman JM. 2010. Whole genome microarray analysis of chicken embryo facial prominences. Dev Dyn 239: 574–591.

Cazorla P, Smidt MP, O'Malley KL, Burbach JP. 2000. A response element for the homeodomain transcription factor Ptx3 in the tyrosine hydroxylase gene promoter. J Neurochem 74:1829–1837.

Chai X, Zhai Y, Napoli JL. 1996. Cloning of a rat cDNA encoding retinol dehydrogenase isozyme type III. Gene 169: 219–222.

Chan T, Satow R, Kitagawa H, Kato S, Asashima M. 2006. Ledgerline, a novel xenopus laevis gene, regulates differentiation of presomitic mesoderm during somitogenesis. Zoolog Sci 23:689–697.

Chepelinsky AB. 2009. Structural function of MIP/aquaporin 0 in the eye lens; genetic defects lead to congenital inherited cataracts. Handb Exp Pharmacol: 265–297.

Cho KW, Blumberg B, Steinbeisser H, De Robertis EM. 1991. Molecular nature of Spemann's organizer: the role of the Xenopus homeobox gene goosecoid. Cell 67:1111–1120.

Cooper DN, Barondes SH. 1999. God must love galectins; he made so many of them. Glycobiology 9:979–984.

Coulon V, L'Honore A, Ouimette JF, Dumontier E, van den Munckhof P, Drouin J. 2007. A muscle-specific promoter directs Pitx3 gene expression in skeletal muscle cells. J Biol Chem 282: 33192–33200.

Cui W, Tomarev SI, Piatigorsky J, Chepelinsky AB, Duncan MK. 2004. Mafs, Prox1, and Pax6 can regulate chicken betaB1-crystallin gene expression. J Biol Chem 279:11088–11095.

Drysdale TA, Elinson RP. 1991. Development of the Xenopus laevis hatching gland and its relationship to surface ectoderm patterning. Development 111: 469–478.

Durston AJ, Timmermans JP, Hage WJ, Hendriks HF, de Vries NJ, Heideveld M, Nieuwkoop PD. 1989. Retinoic acid causes an anteroposterior transformation in the developing central nervous system. Nature 340:140–144.

Dutta S, Dietrich JE, Aspock G, Burdine RD, Schier A, Westerfield M, Varga ZM. 2005. pitx3 defines an equivalence domain for lens and anterior pituitary placode. Development 132:1579–1590.

Eisen JS, Smith JC. 2008. Controlling morpholino experiments: don't stop making antisense. Development 135: 1735–1743.

Engstrom PG, Fredman D, Lenhard B. 2008. Ancora: a web resource for exploring highly conserved noncoding elements and their association with developmental regulatory genes. Genome Biol 9:R34.

Flower DR. 1996. The lipocalin protein family: structure and function. Biochem J 318(pt 1):1–14.

Goodman DS. 1981. Retinoid-binding proteins in plasma and in cells. Ann N Y Acad Sci 359:69–78.

Gray IC, Fallowfield J, Ford S, Nobile C, Volpi EV, Spurr NK. 1997. An integrated physical and genetic map spanning chromosome band 10q24. Genomics 43:85–88.

Halder G, Callaerts P, Gehring WJ. 1995. Induction of ectopic eyes by targeted expression of the eyeless gene in Drosophila. [see comments]. Science 267: 1788–1792.

Harland RM. 1991. In situ hybridization: an improved whole-mount method for Xenopus embryos. Methods Cell Biol 36:685–695.

Hitachi K, Danno H, Tazumi S, Aihara Y, Uchiyama H, Okabayashi K, Kondow A, Asashima M. 2009. The Xenopus Bowline/Ripply family proteins negatively regulate the transcriptional activity of T-box transcription factors. Int J Dev Biol 53:631–639.

Ho HY, Chang KH, Nichols J, Li M. 2009. Homeodomain protein Pitx3 maintains the mitotic activity of lens epithelial cells. Mech Dev 126:18–29.

Huang B, He W. 2010. Molecular characteristics of inherited congenital cataracts. Eur J Med Genet 53:347–357.

Hwang DY, Hong S, Jeong JW, Choi S, Kim H, Kim J, Kim KS. 2009. Vesicular monoamine transporter 2 and dopamine transporter are molecular targets of Pitx3 in the ventral midbrain dopamine neurons. J Neurochem 111:1202–1212.

Isaacs HV, Tannahill D, Slack JM. 1992. Expression of a novel FGF in the Xenopus embryo. A new candidate inducing factor for mesoderm formation and anteroposterior specification. Development 114:711–720.

Isaacs HV, Pownall ME, Slack JMW. 1994. eFGF regulates Xbra expression during Xenopus gastrulation. EMBO J 13:4469–4481.

Ishibashi S, Yasuda K. 2001. Distinct roles of maf genes during Xenopus lens development. Mech Dev 101:155–166.

Ito T, Levenstein ME, Fyodorov DV, Kutach AK, Kobayashi R, Kadonaga JT. 1999. ACF consists of two subunits, Acf1 and ISWI, that function cooperatively in the ATP-dependent catalysis of chromatin assembly. Genes Dev 13: 1529–1539.

Jacobs FM, Smits SM, Noorlander CW, von Oerthel L, van der Linden AJ, Burbach JP, Smidt MP. 2007. Retinoic acid counteracts developmental defects in the substantia nigra caused by Pitx3 deficiency. Development 134:2673–2684.

Jen WC, Gawantka V, Pollet N, Niehrs C, Kintner C. 1999. Periodic repression of Notch pathway genes governs the segmentation of Xenopus embryos. Genes Dev 13:1486–1499.

Jones MH, Hamana N, Nezu J, Shimane M. 2000a. A novel family of bromodomain genes. Genomics 63:40–45.

Jones MH, Hamana N, Shimane M. 2000b. Identification and characterization of BPTF, a novel bromodomain transcription factor. Genomics 63:35–39.

Kameda Y, Saitoh T, Fujimura T. 2011. Hes1 regulates the number and anterior-posterior patterning of mesencephalic dopaminergic neurons at the mid/hindbrain boundary (isthmus). Dev Biol 358:91–101.

Kawamura A, Koshida S, Takada S. 2008. Activator-to-repressor conversion of T-box transcription factors by the Ripply family of Groucho/TLE-associated mediators. Mol Cell Biol 28:3236–3244.

Khosrowshahian F, Wolanski M, Chang WY, Fujiki K, Jacobs L, Crawford MJ. 2005. Lens and retina formation require expression of Pitx3 in Xenopus pre-lens ectoderm. Dev Dyn 234:577–589.

Kikuta H, Laplante M, Navratilova P, Komisarczuk AZ, Engstrom PG, Fredman D, Akalin A, Caccamo M, Sealy I, Howe K, Ghislain J, Pezeron G, Mourrain P, Ellingsen S, Oates AC, Thisse C, Thisse B, Foucher I, Adolf B, Geling A, Lenhard B, Becker TS. 2007. Genomic regulatory blocks encompass multiple neighboring genes and maintain conserved synteny in vertebrates. Genome Res 17:545–555.

Ladher R, Mohun TJ, Smith JC, Snape AM. 1996. Xom: a Xenopus homeobox gene that mediates the early effects of BMP-4. Development 122:2385–2394.

Lamonerie T, Trembley J, Lanctot C, Therrien M, Gautier Y, Drouin J. 1996. Ptx1, a bicoid-related homeo box transcription factor involved in the transcription of the pro-opiomelanocortin gene. Genes Dev 10:1284–1295.

Landis SC, Siegel RE, Schwab M. 1988. Evidence for neurotransmitter plasticity in vivo. II. Immunocytochemical studies of rat sweat gland innervation during development. Dev Biol 126:129–140.

Lebel M, Gauthier Y, Moreau A, Drouin J. 2001. Pitx3 activates mouse tyrosine hydroxylase promoter via a high-affinity binding site. J Neurochem 77:558–567.

Lombardo A, Slack JM. 2001. Abdominal B-type Hox gene expression in Xenopus laevis. Mech Dev 106:191–195.

Marchand R, Poirier LJ. 1983. Isthmic origin of neurons of the rat substantia nigra. Neuroscience 9:373–381.

Messmer K, Remington MP, Skidmore F, Fishman PS. 2007. Induction of tyrosine hydroxylase expression by the transcription factor Pitx3. Int J Dev Neurosci 25:29–37.

Mochizuki T, Karavanov AA, Curtiss PE, Ault KT, Sugimoto N, Watabe T, Shiokawa K, Jamrich M, Cho KW, Dawid IB, Taira M. 2000. Xlim-1 and LIM domain binding protein 1 cooperate with various transcription factors in the regulation of the goosecoid promoter. Dev Biol 224:470–485.

Münster D. 2005. Pitx3 und seine Rolle in der Augen- und Gehirnentwicklung. In: GSF-Forschungszentrum für Umwelt und Gesundheit Institut für Entwicklungsgenetik Neuherberg: Technischen Universität München. p 115.

Murato Y, Nagatomo K, Yamaguti M, Hashimoto C. 2007. Two alloalleles of Xenopus laevis hairy2 gene–evolution of duplicated gene function from a developmental perspective. Dev Genes Evol 217:665–673.

Nagy L, Saydak M, Shipley N, Lu S, Basilion JP, Yan ZH, Syka P, Chandraratna RA, Stein JP, Heyman RA, Davies PJ. 1996. Identification and characterization of a versatile retinoid response element (retinoic acid receptor response element-retinoid X receptor response element) in the mouse tissue transglutaminase gene promoter. J Biol Chem 271:4355–4365.

Nakamura H, Watanabe Y. 2005. Isthmus organizer and regionalization of the mesencephalon and metencephalon. Int J Dev Biol 49:231–235.

Napoli JL, Posch KP, Fiorella PD, Boerman MHEM. 1991. Physiological occurrence, biosynthesis and metabolism of retinoic acid: evidence for roles of cellular retinol-binding protein (CRBP) and cellular retinoic acid-binding protein (CRABP) in the pathway of retinoic acid homeostasis. Biomed Pharmacother 45:131–143.

Nieuwkoop PD, Faber J. 1967. Normal Table of Xenopus laevis (Daudin). Amsterdam: North Holland Press.

Ossipova O, Stick R, Pieler T. 2002. XSPR-1 and XSPR-2, novel Sp1 related zinc finger containing genes, are dynamically expressed during Xenopus embryogenesis. Mech Dev 115:117–122.

Pares X, Farres J, Kedishvili N, Duester G. 2008. Medium- and short-chain dehydrogenase/reductase gene and protein families: medium-chain and short-chain dehydrogenases/reductases in retinoid metabolism. Cell Mol Life Sci 65:3936–3949.

Pommereit D, Pieler T, Hollemann T. 2001. Xpitx3: a member of the Rieg/Pitx gene family expressed during pituitary and lens formation in Xenopus laevis. Mech Dev 102:255–257.

Reza HM, Ogino H, Yasuda K. 2002. L-Maf, a downstream target of Pax6, is essential for chick lens development. Mech Dev 116:61–73.

Rieger DK, Reichenberger E, McLean W, Sidow A, Olsen BR. 2001. A double-deletion mutation in the pitx3 gene causes arrested lens development in aphakia mice. Genomics 72:61–72.

Sakazume S, Sorokina E, Iwamoto Y, Semina EV. 2007. Functional analysis of human mutations in homeodomain transcription factor PITX3. BMC Mol Biol 8:84.

Semina EV, Murray JC, Reiter R, Hrstka RF, Graw J. 2000. Deletion in the promoter region and altered expression of Pitx3 homeobox gene in aphakia mice. Hum Mol Genet 9:1575–1585.

Shawlot W, Behringer RR. 1995. Requirement for Lim1 in head-organizer function. [see comments]. Nature 374:425–430.

Shi X, Bosenko DV, Zinkevich NS, Foley S, Hyde DR, Semina EV, Vihtelic TS. 2005. Zebrafish pitx3 is necessary for normal lens and retinal development. Mech Dev 122:513–527.

Shinga J, Itoh M, Shiokawa K, Taira S, Taira M. 2001. Early patterning of the

prospective midbrain-hindbrain boundary by the HES-related gene XHR1 in Xenopus embryos. Mech Dev 109:225–239.

Shoji H, Nishi N, Hirashima M, Nakamura T. 2003. Characterization of the Xenopus galectin family. Three structurally different types as in mammals and regulated expression during embryogenesis. J Biol Chem 278:12285–12293.

Simon A, Hellman U, Wernstedt C, Eriksson U. 1995. The retinal pigment epithelial-specific 11-cis retinol dehydrogenase belongs to the family of short chain alcohol dehydrogenases. J Biol Chem 270:1107–1112.

Simon A, Lagercrantz J, Bajalica-Lagercrantz S, Eriksson U. 1996. Primary structure of human 11-cis retinol dehydrogenase and organization and chromosomal localization of the corresponding gene. Genomics 36:424–430.

Smoczer C, Hooker L, Brode S, Wolanski M, KhosrowShahian F, Crawford M. (In Press). The Xenopus homeobox gene Pitx3 impinges upon somitogenesis and laterality. Biochem Cell Biol.

Sorokina EA, Muheisen S, Mlodik N, Semina EV. 2011. MIP/Aquaporin 0 represents a direct transcriptional target of PITX3 in the developing lens. PLoS One 6:e21122.

Tada M, Casey ES, Fairclough L, Smith JC. 1998. Bix1, a direct target of Xenopus T-box genes, causes formation of ventral mesoderm and endoderm. Development 125:3997–4006.

Takada H, Hattori D, Kitayama A, Ueno N, Taira M. 2005. Identification of target genes for the Xenopus Hes-related protein XHR1, a prepattern factor specifying the midbrain-hindbrain boundary. Dev Biol 283:253–267.

Tanaka M, Murayama D, Nagashima M, Higashi T, Mawatari K, Matsukawa T, Kato S. 2007. Purpurin expression in the zebrafish retina during early development and after optic nerve lesion in adults. Brain Res 1153: 34–42.

Trindade M, Tada M, Smith JC. 1999. DNA-binding specificity and embryological function of Xom (Xvent-2). Dev Biol 216:442–456.

Tsuji S, Cho KW, Hashimoto C. 2003. Expression pattern of a basic helix-loop-helix transcription factor Xhairy2b during Xenopus laevis development. Dev Genes Evol 213:407–411.

van den Munckhof P, Luk KC, Ste-Marie L, Montgomery J, Blanchet PJ, Sadikot AF, Drouin J. 2003. Pitx3 is required for motor activity and for survival of a subset of midbrain dopaminergic neurons. Development 130: 2535–2542.

Varnum DS, Stevens LC. 1968. Aphakia, a new mutation in the mouse. J Hered 59:147–150.

Wald G. 1968. The molecular basis of visual excitation. Nature 219:800–807.

Wolda SL, Moon RT. 1992. Cloning and developmental expression in Xenopus laevis of seven additional members of the Wnt family. Oncogene 7: 1941–1947.

Würst W, Auerbach AB, Joyner AL. 1994. Multiple developmental defects in Engrailed-1 mutant mice: an early mid-hindbrain deletion and patterning defects in forlimbs and sternum. Developement 120:2065–2075.

Zeng L, Zhou MM. 2002. Bromodomain: an acetyl-lysine binding domain. FEBS Lett 513:124–128.